Electronic Supplementary Material (ESI) for Organic & Biomolecular Chemistry.
This journal is © The Royal Society of Chemistry 2020

Establishing linear-free-energy relationships for the quadricyclane-to-norbornadiene reaction

Mads Mansø,[a,b] Anne Ugleholdt Petersen,[a] Kasper Moth-Poulsen[b] and Mogens Brøndsted Nielsen[a,*]

[a] *Department of Chemistry, University of Copenhagen, Universitetsparken 5, DK-2100 Copenhagen Ø, Denmark. E-mail: mbn@chem.ku.dk*
[b] *Department of Chemistry and Chemical Engineering, Chalmers University of Technology, Kemivägen 10, 412 96 Gothenburg, Sweden*

ELECTRONIC SUPPLEMENTARY INFORMATION

CONTENTS

NMR Spectra

Compound NBD12

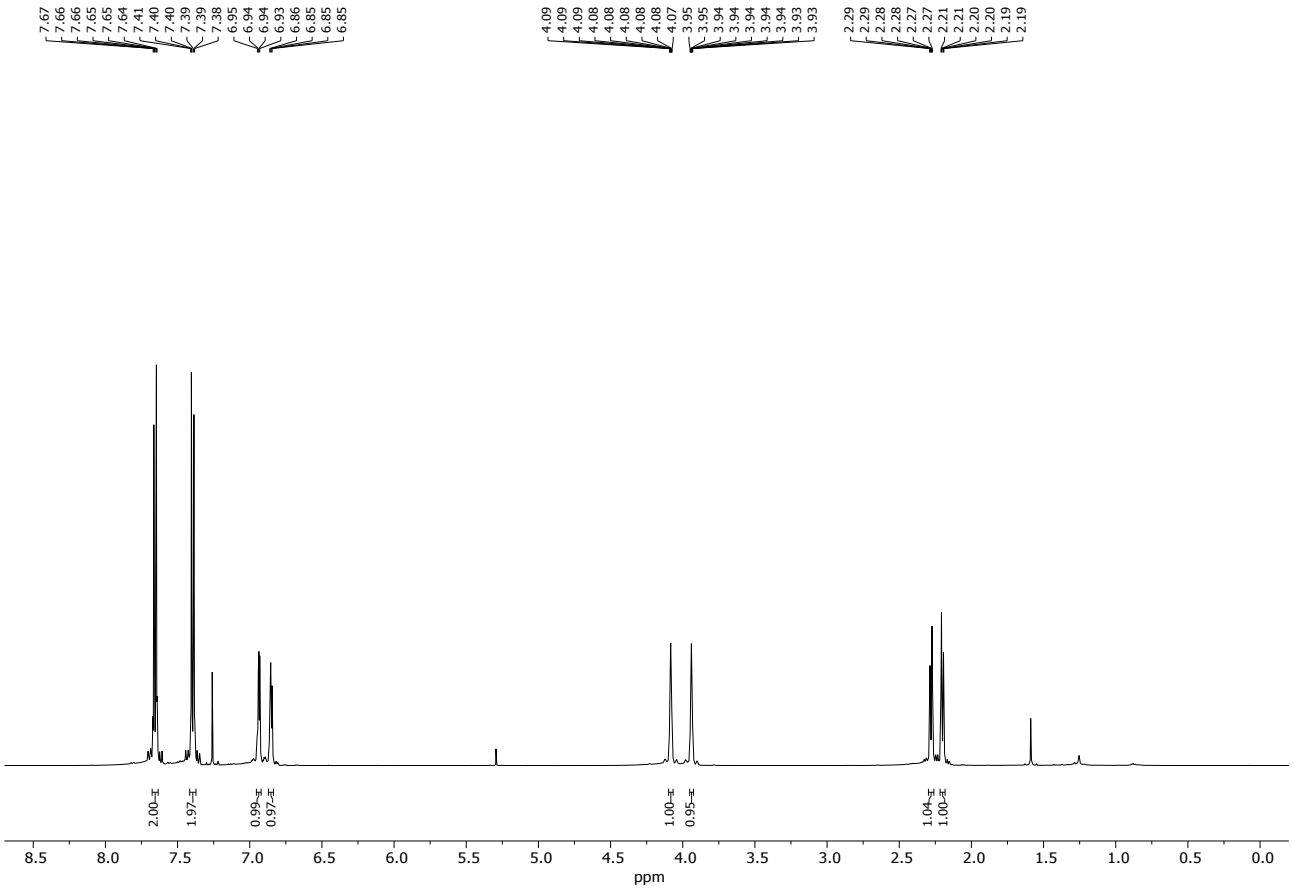

Figure S1: ^{1}H NMR (500 MHz) of **NBD12** in $CDCl_3$.

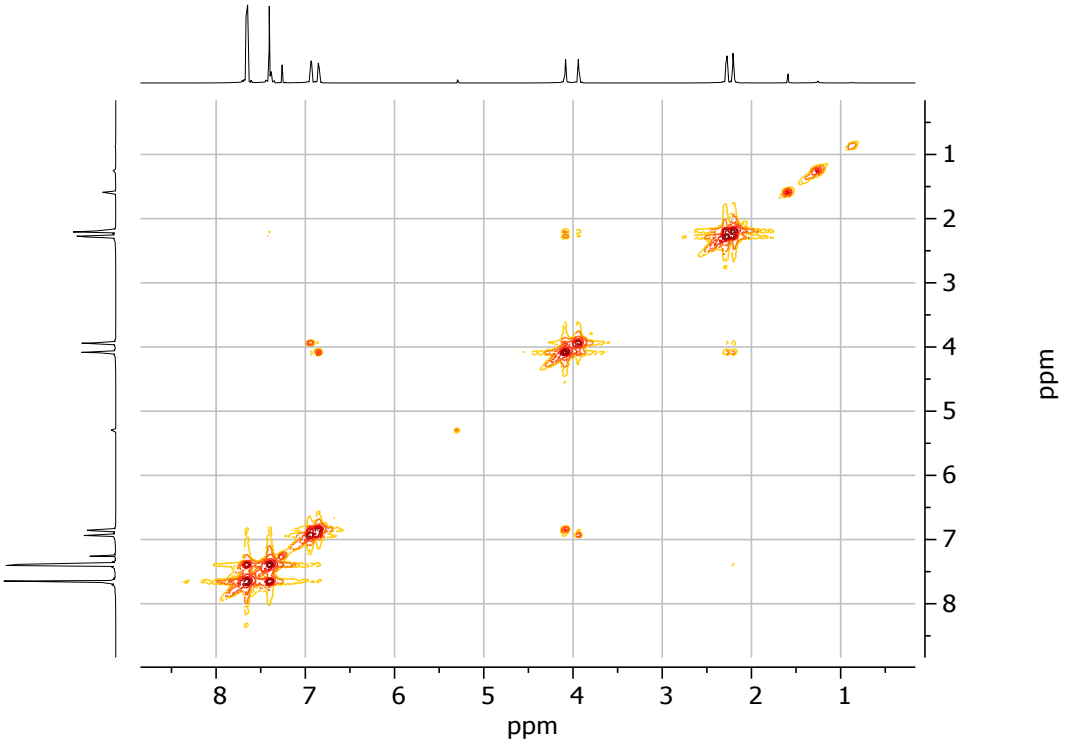

Figure S2: COSY NMR (500 MHz) of **NBD12** in $CDCl_3$.

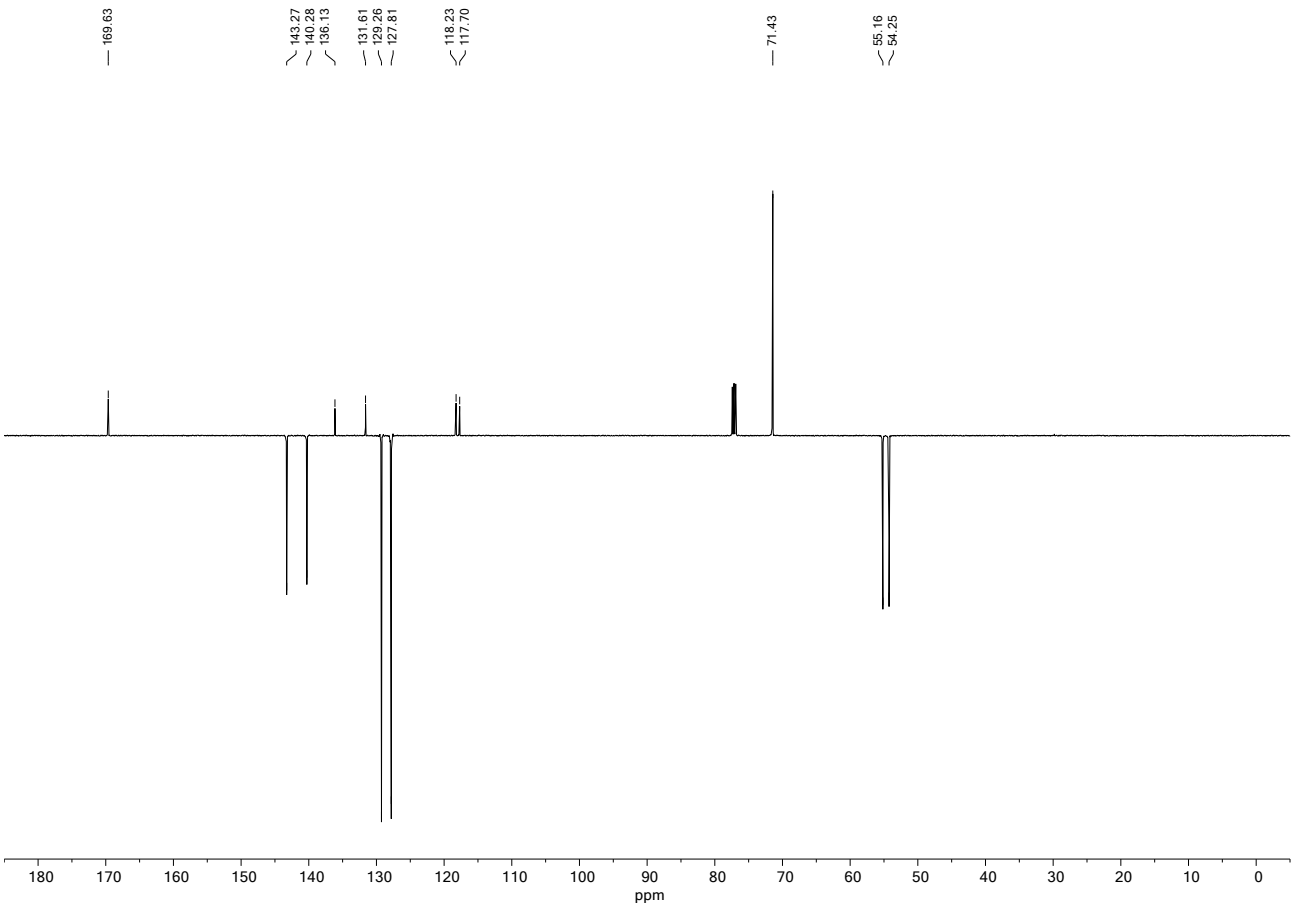

Figure S3: ^{13}C APT NMR (126 MHz) of **NBD12** in $CDCl_3$.

Compound NBD13

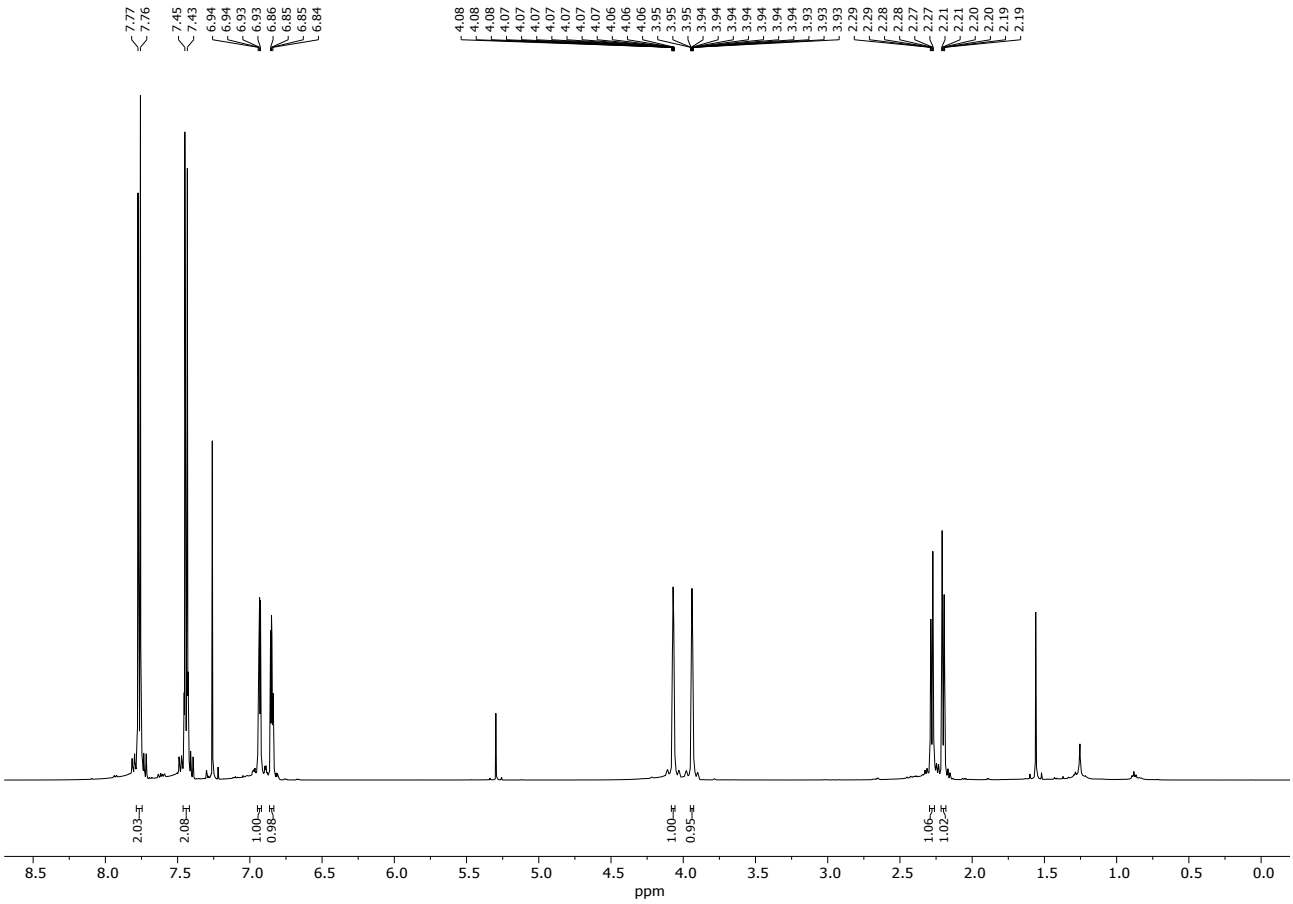

Figure S4: ^{1}H NMR (500 MHz) of **NBD13** in $CDCl_3$.

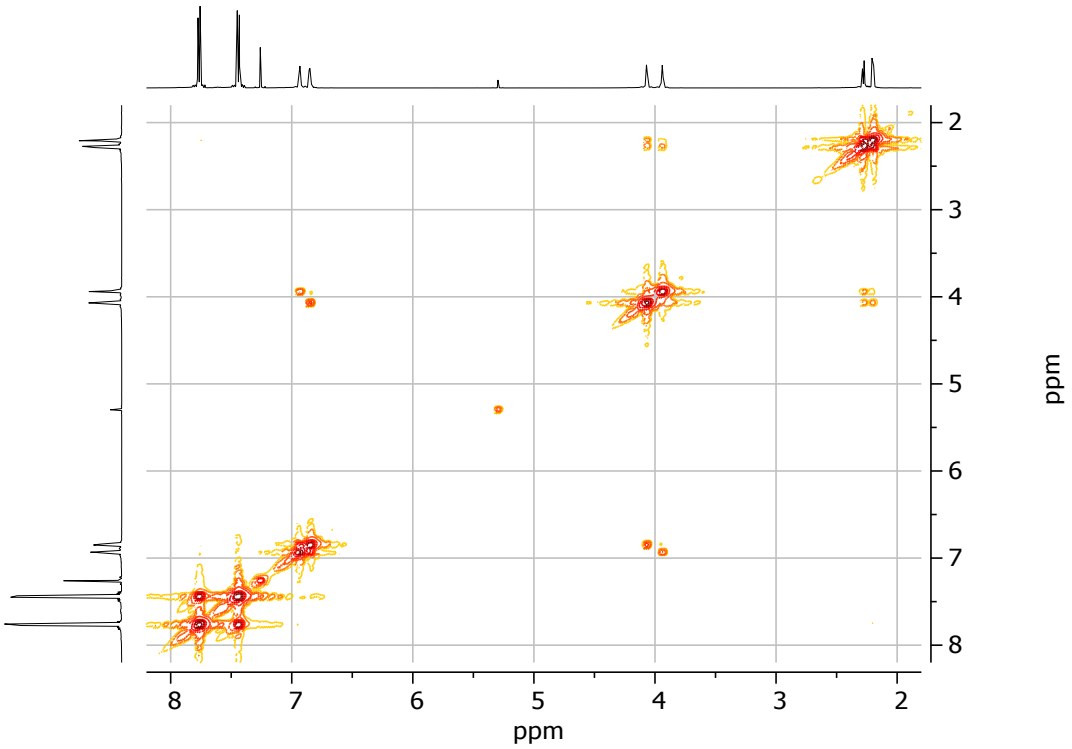

Figure S5: COSY NMR (500 MHz) of **NBD13** in $CDCl_3$.

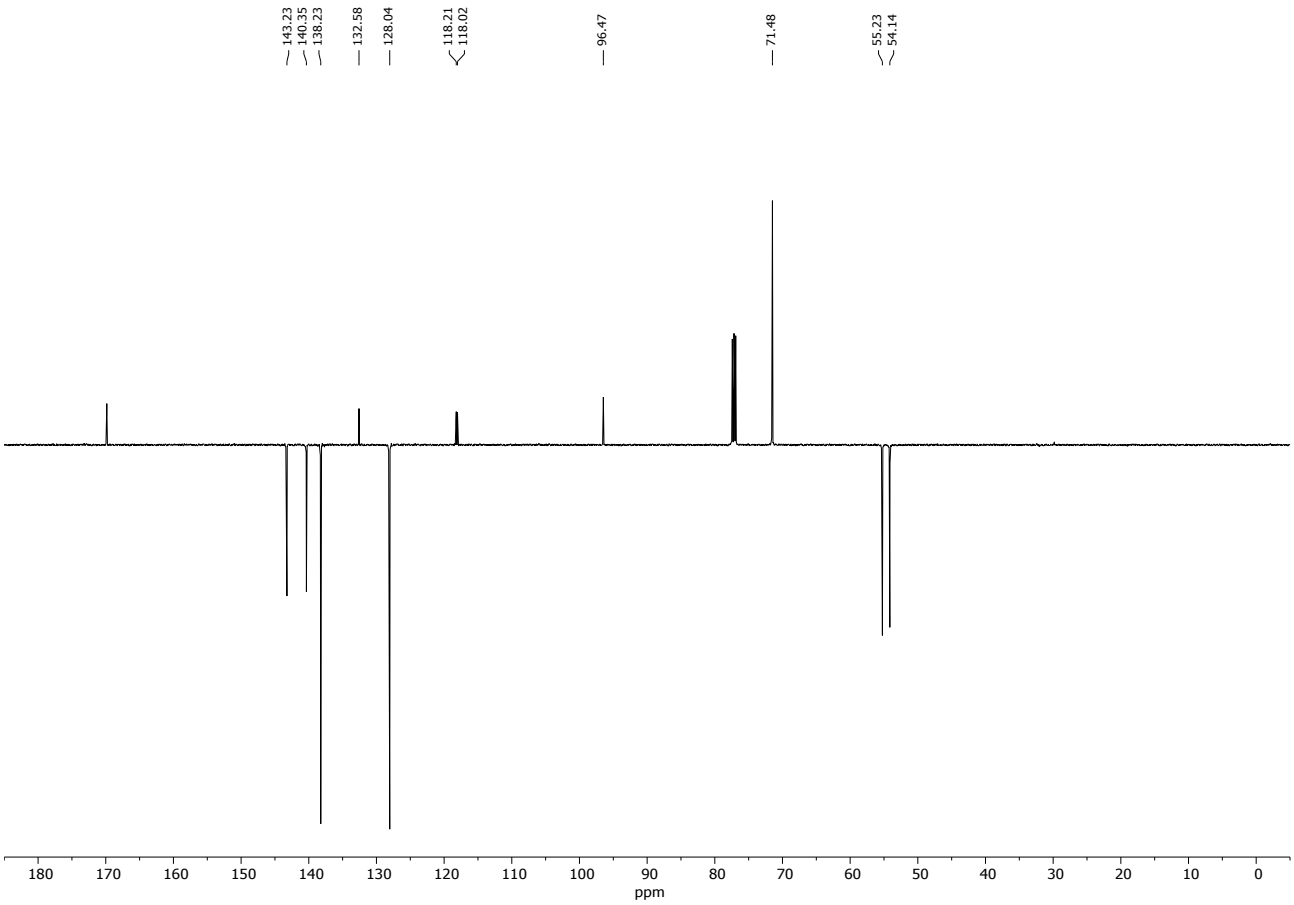

Figure S6: ^{13}C APT NMR (126 MHz) of **NBD13** in $CDCl_3$.

Compound NBD14

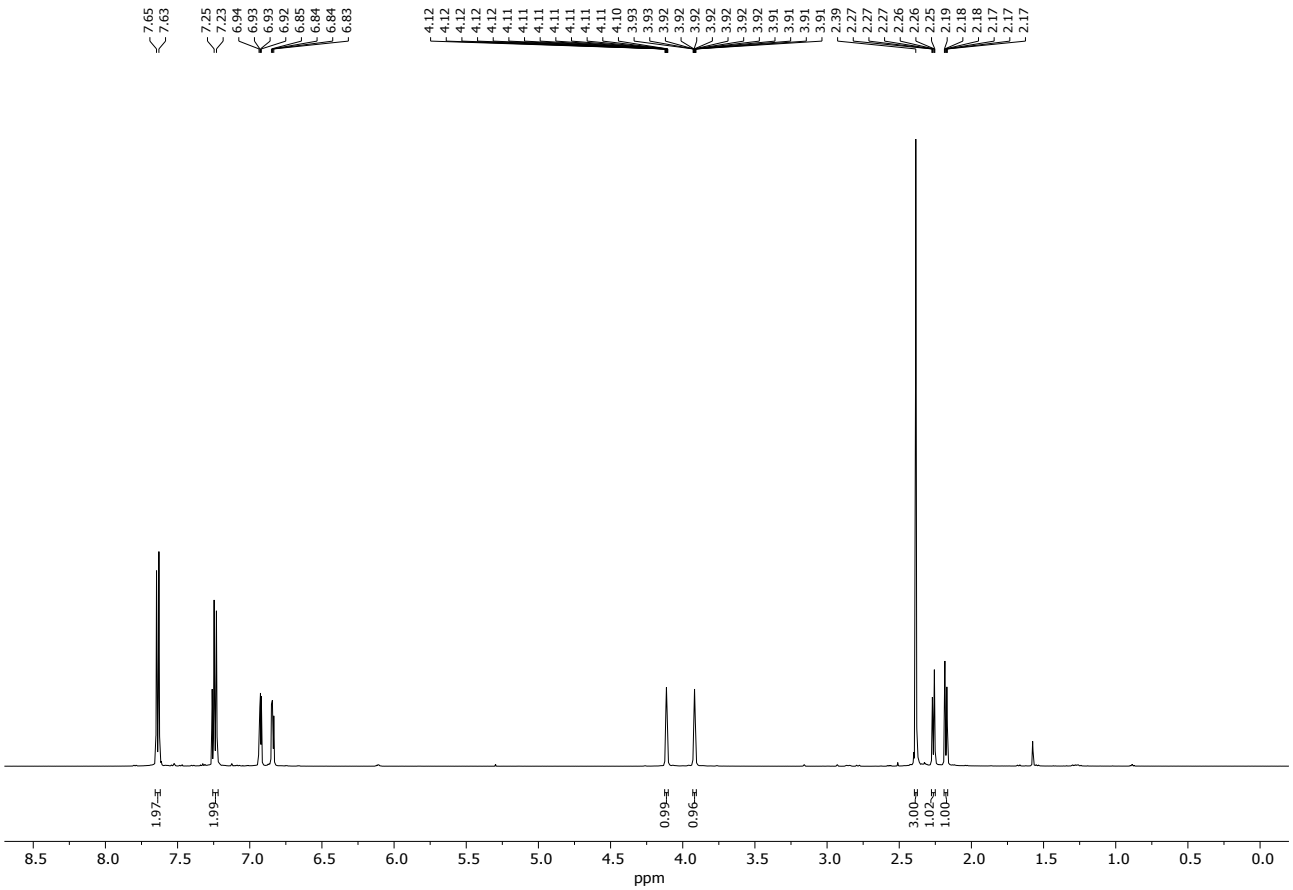

Figure S7: ^{1}H NMR (500 MHz) of **NBD14** in $CDCl_3$.

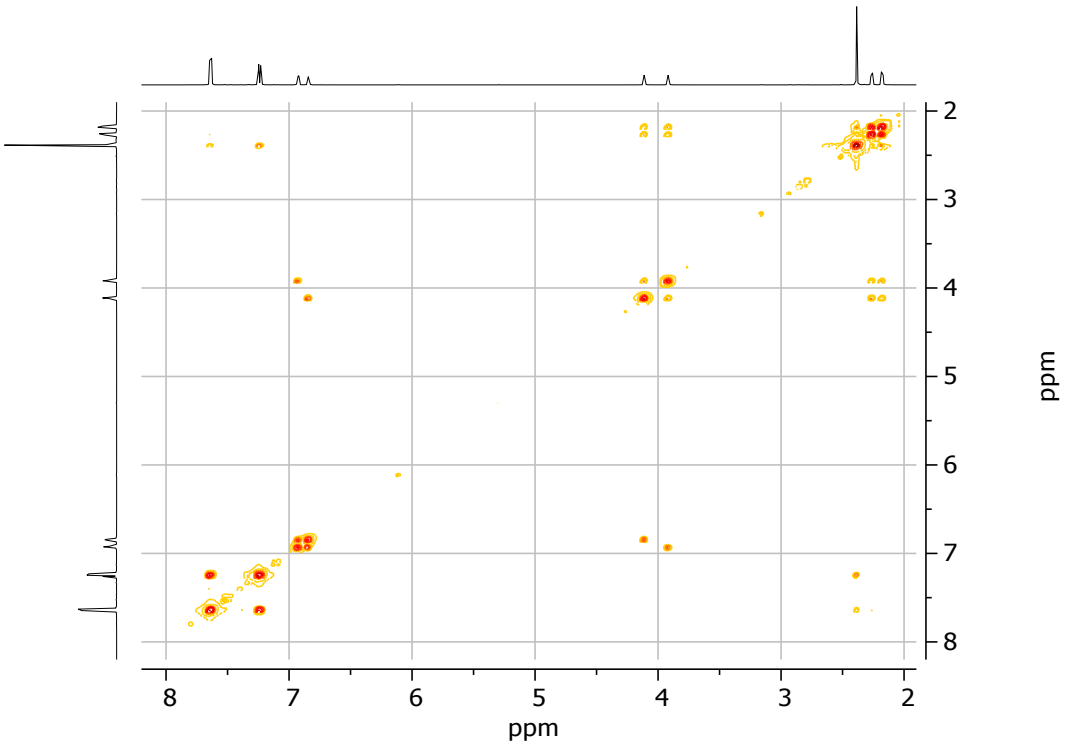

Figure S8: COSY NMR (500 MHz) of **NBD14** in $CDCl_3$.

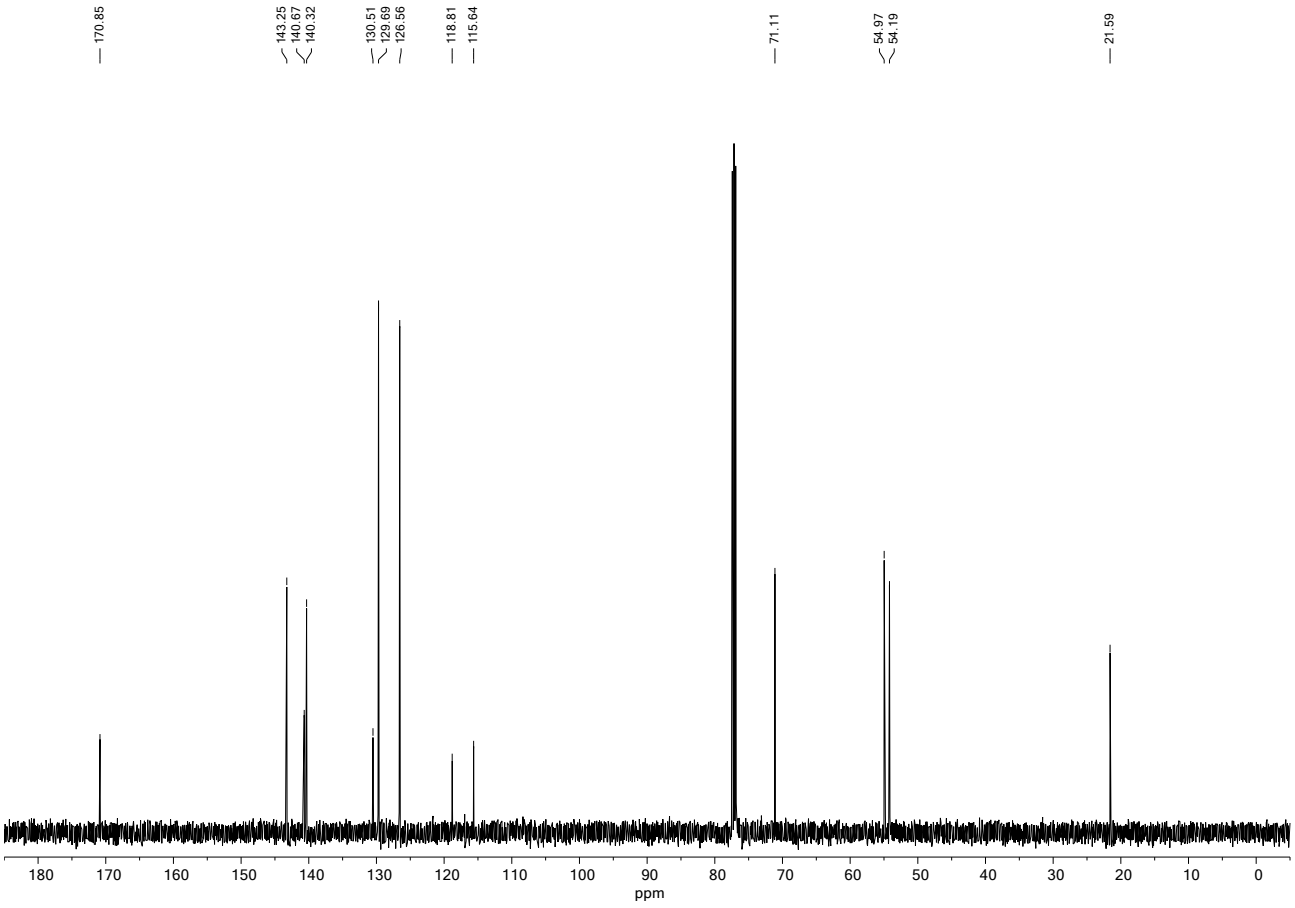

Figure S9: ^{13}C NMR (126 MHz) of **NBD14** in $CDCl_3$.

Compound NBD15

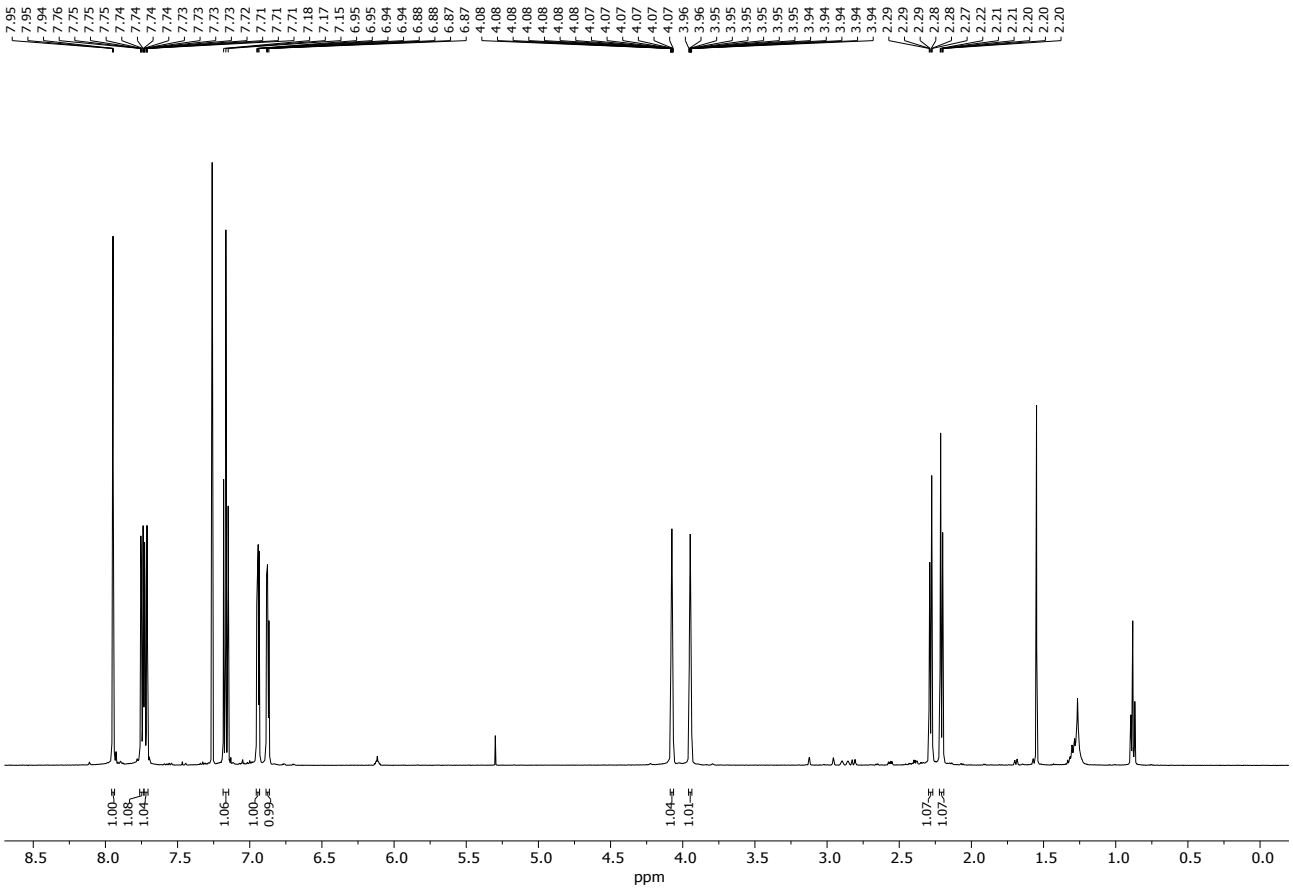

Figure S10: ^{1}H NMR (500 MHz) of **NBD15** in $CDCl_3$.

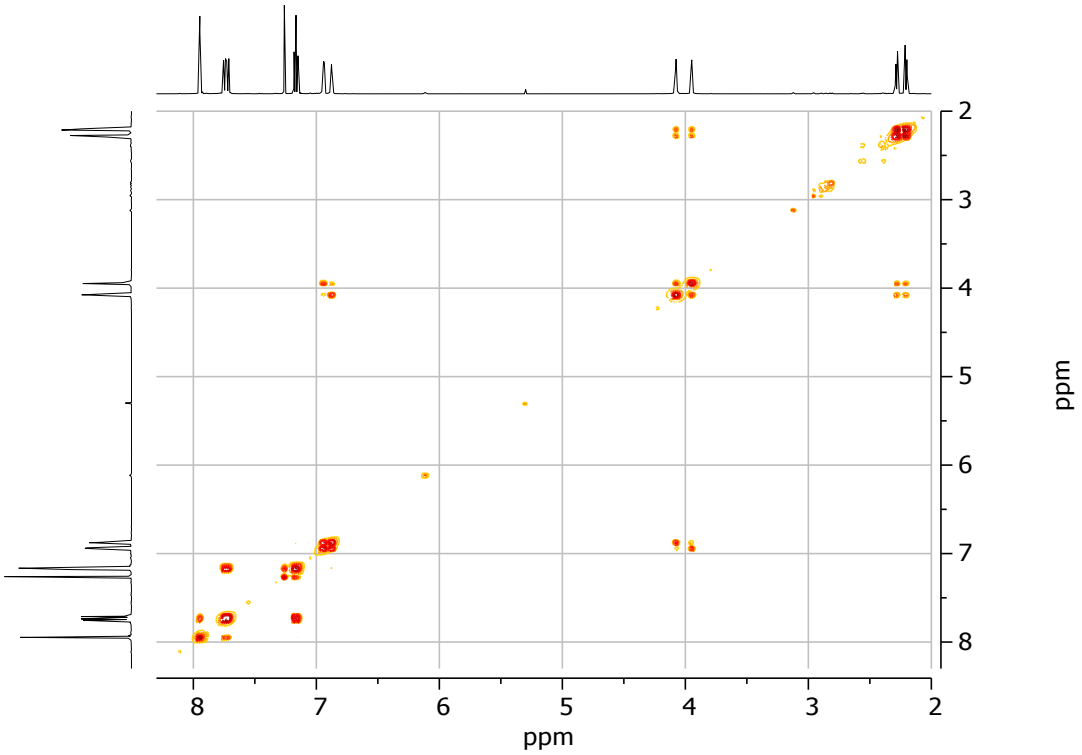

Figure S11: COSY NMR (500 MHz) of **NBD15** in $CDCl_3$.

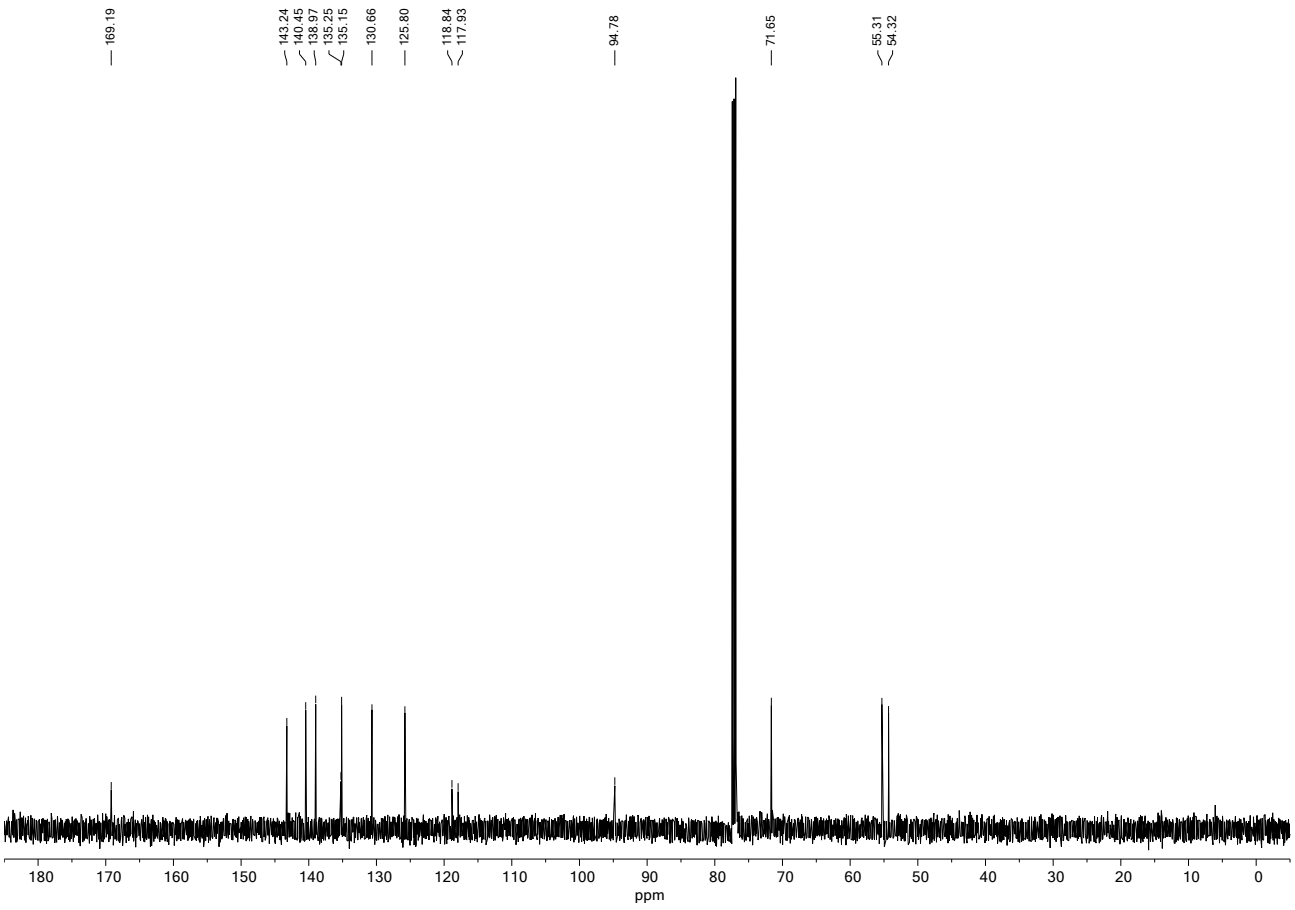

Figure S12: ^{13}C NMR (126 MHz) of **NBD15** in $CDCl_3$.

Compound NBD16

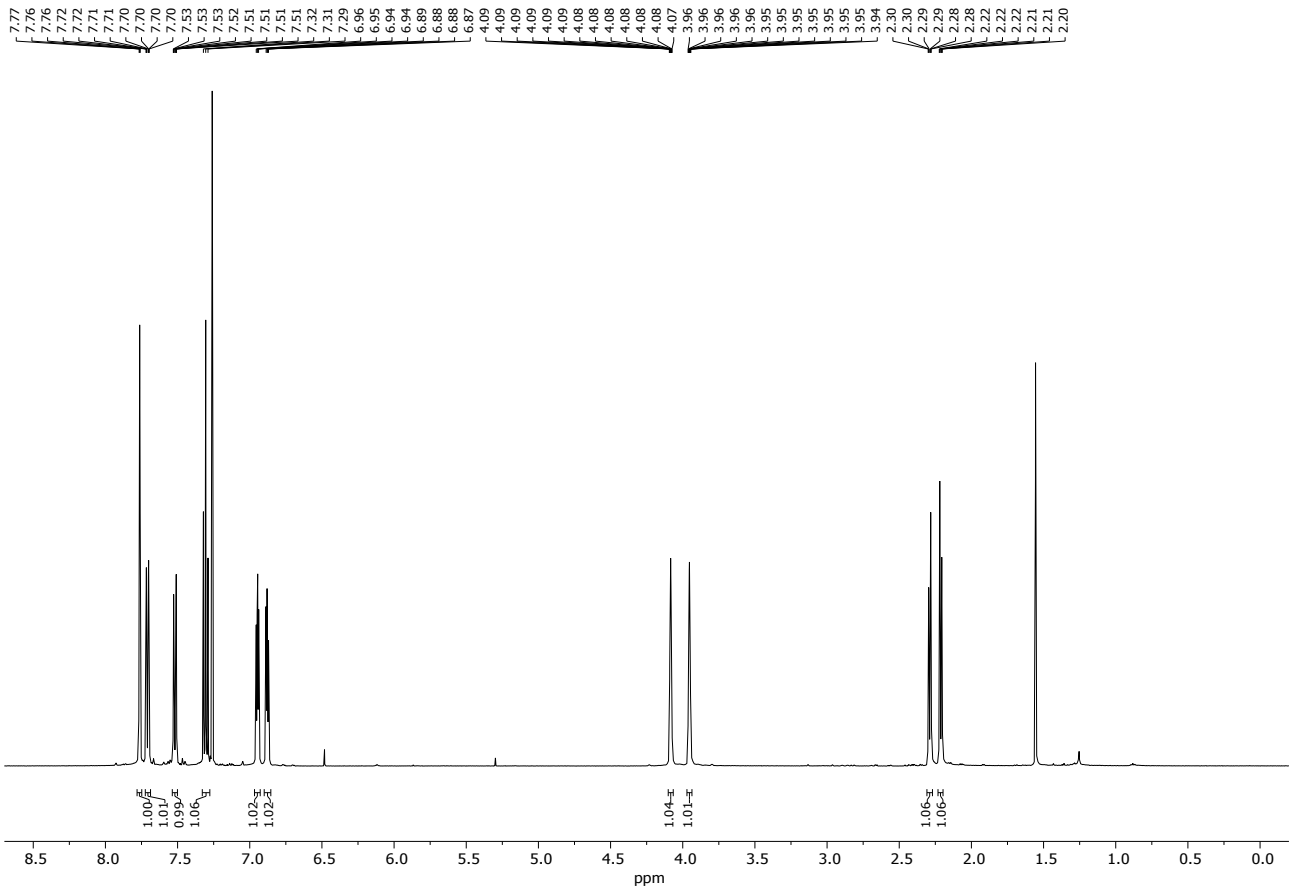

Figure S13: ^{1}H NMR (500 MHz) of **NBD16** in $CDCl_3$.

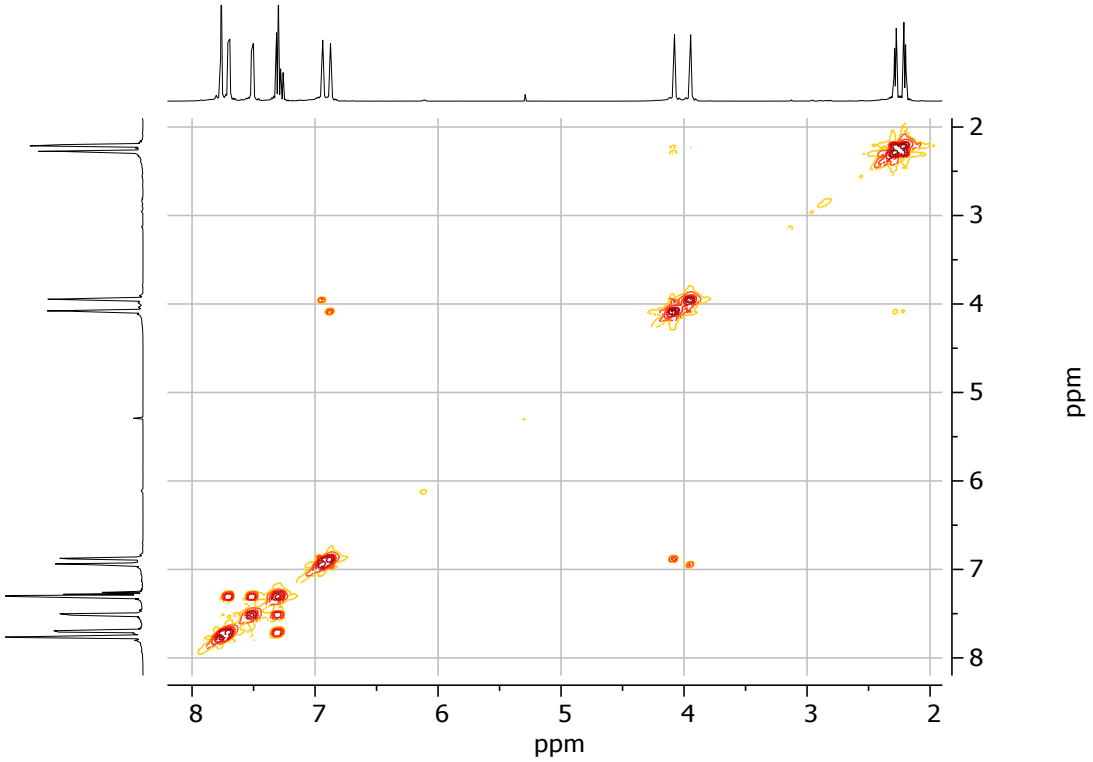

Figure S14: COSY NMR (500 MHz) of **NBD16** in $CDCl_3$.

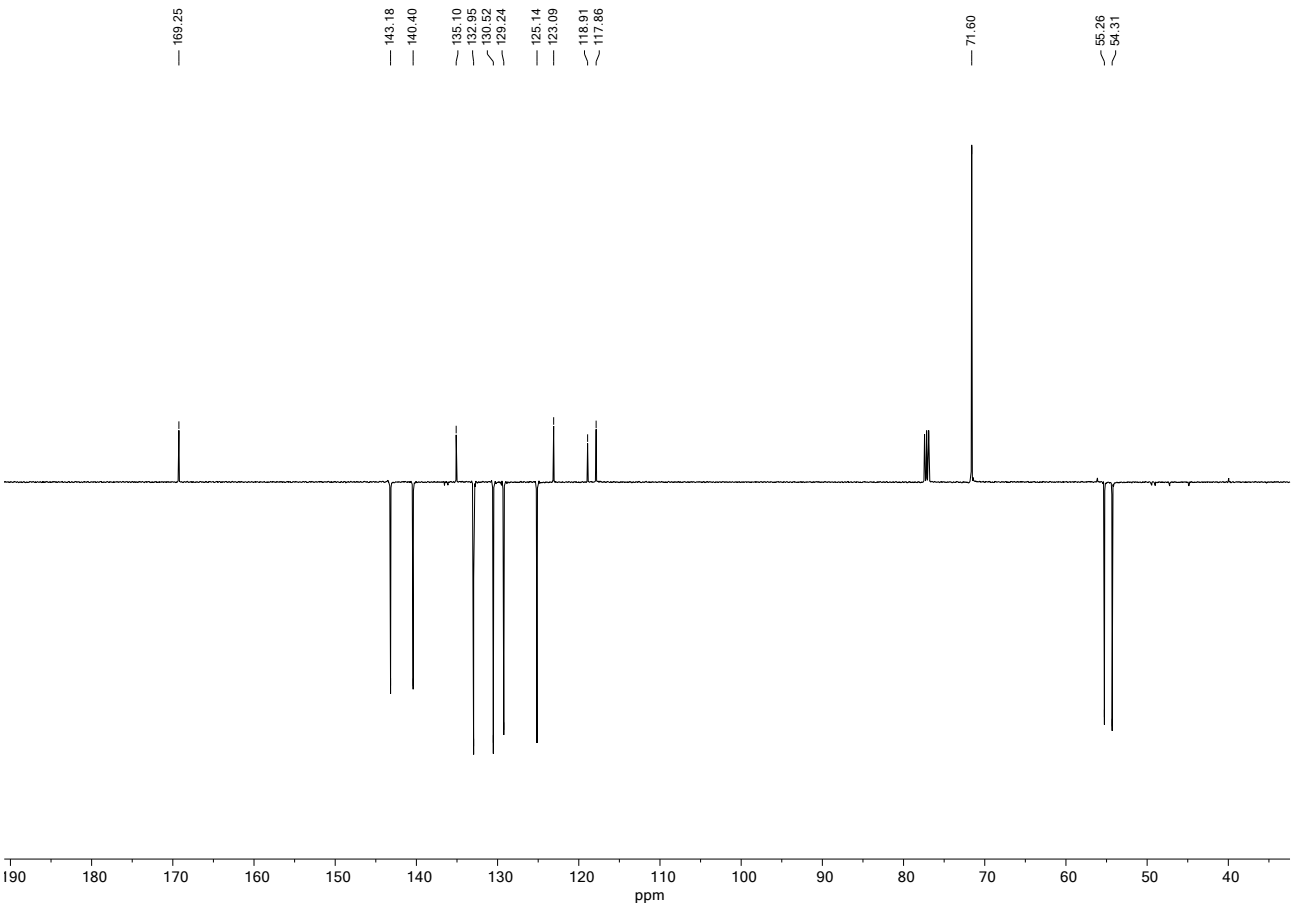

Figure S15: ^{13}C APT NMR (126 MHz) of **NBD16** in $CDCl_3$.

Compound NBD17

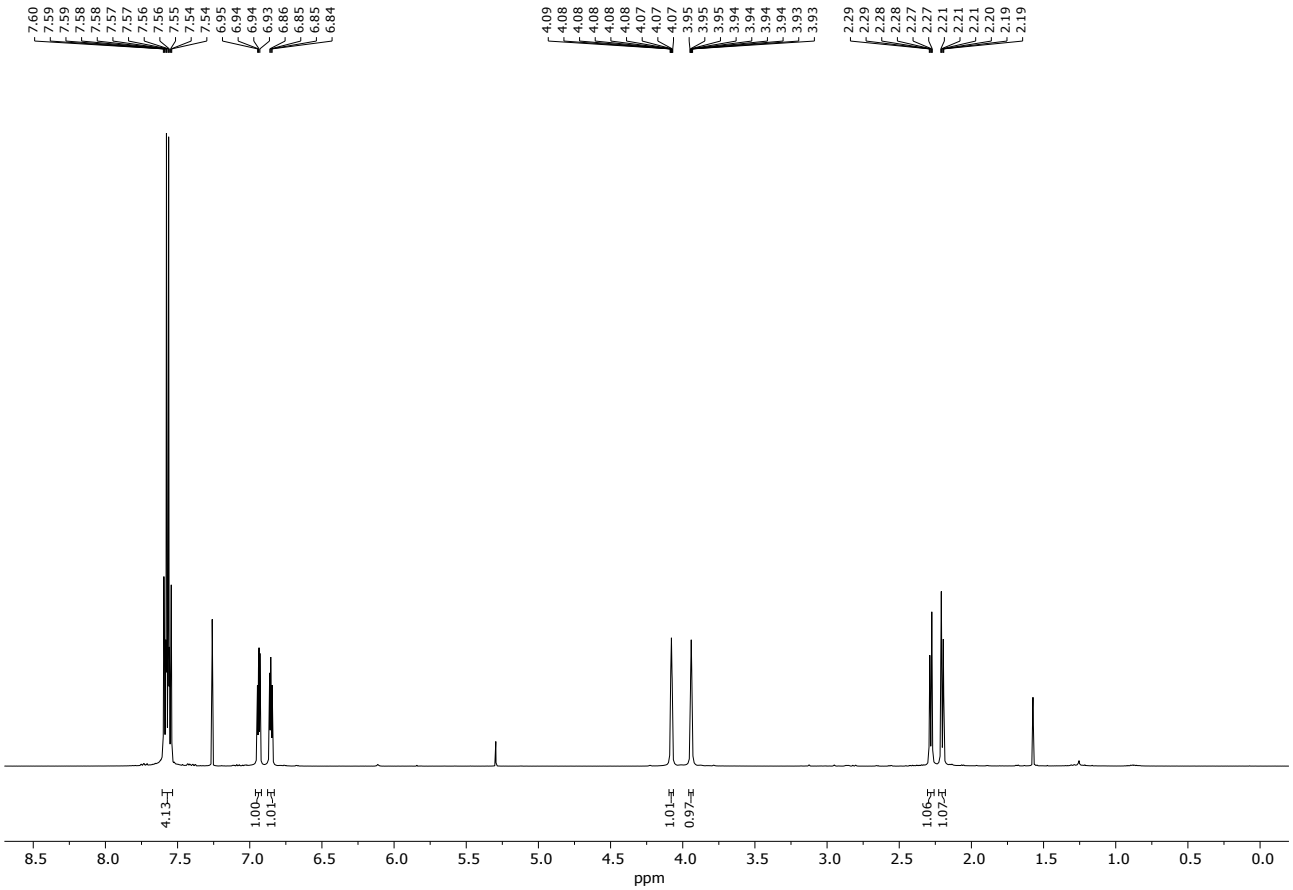

Figure S16: ^{1}H NMR (400 MHz) of **NBD17** in $CDCl_3$.

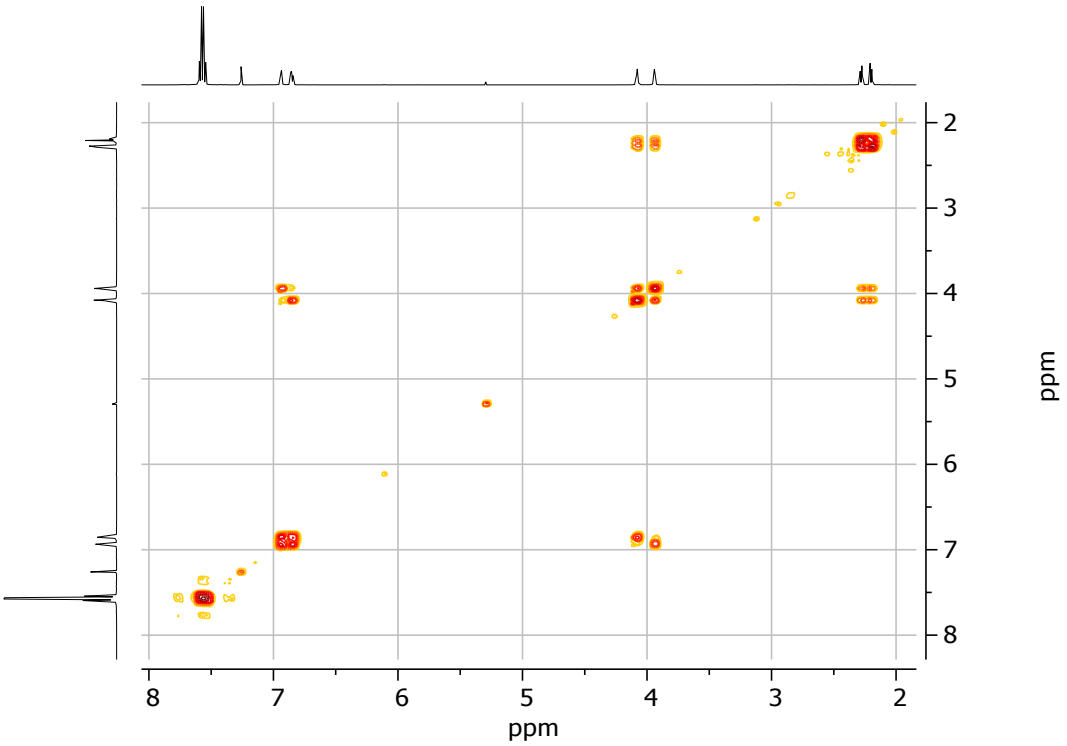

Figure S17: COSY NMR (400 MHz) of **NBD17** in $CDCl_3$.

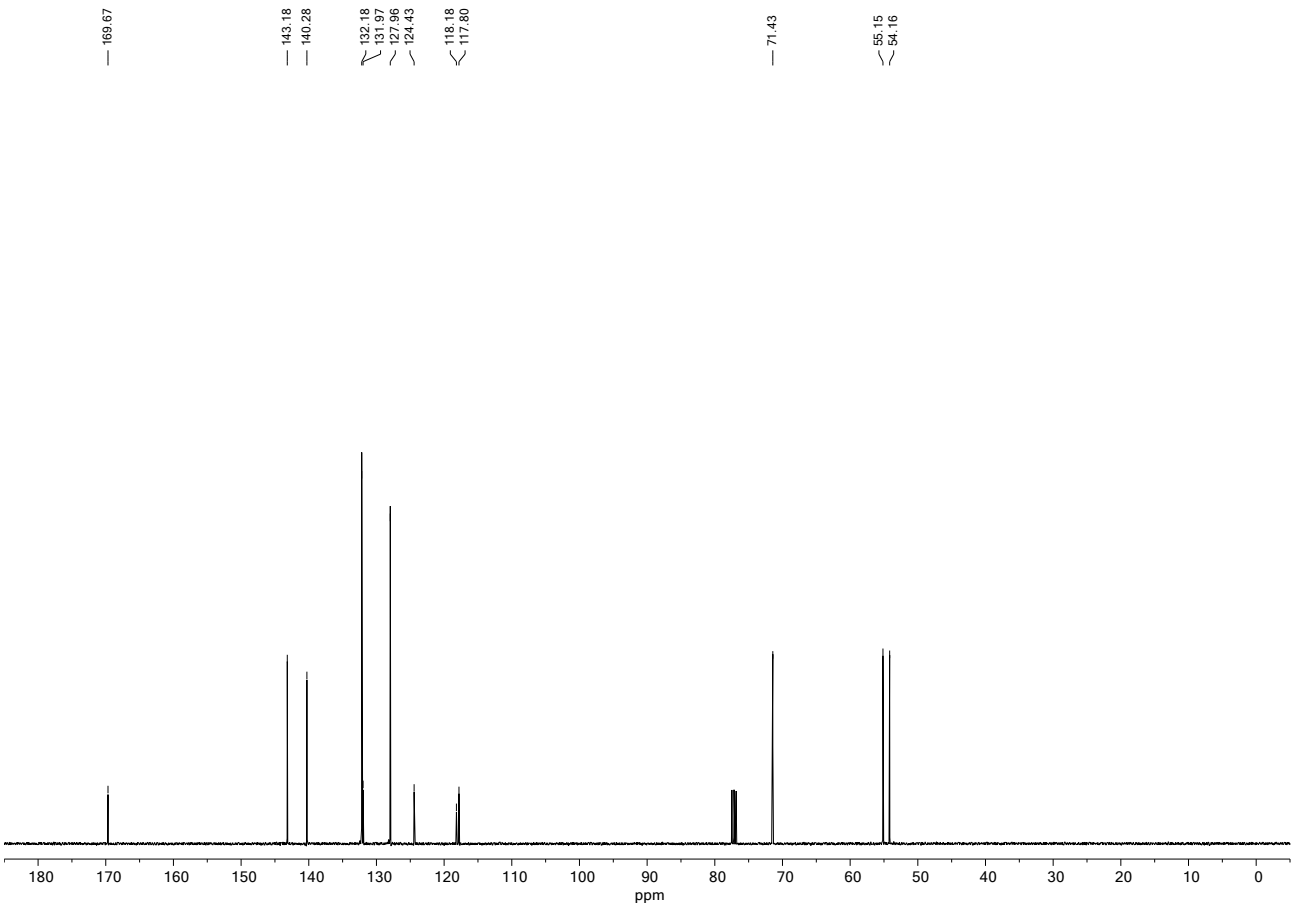

Figure S18: ^{13}C NMR (100 MHz) of **NBD17** in $CDCl_3$.

Compound NBD18

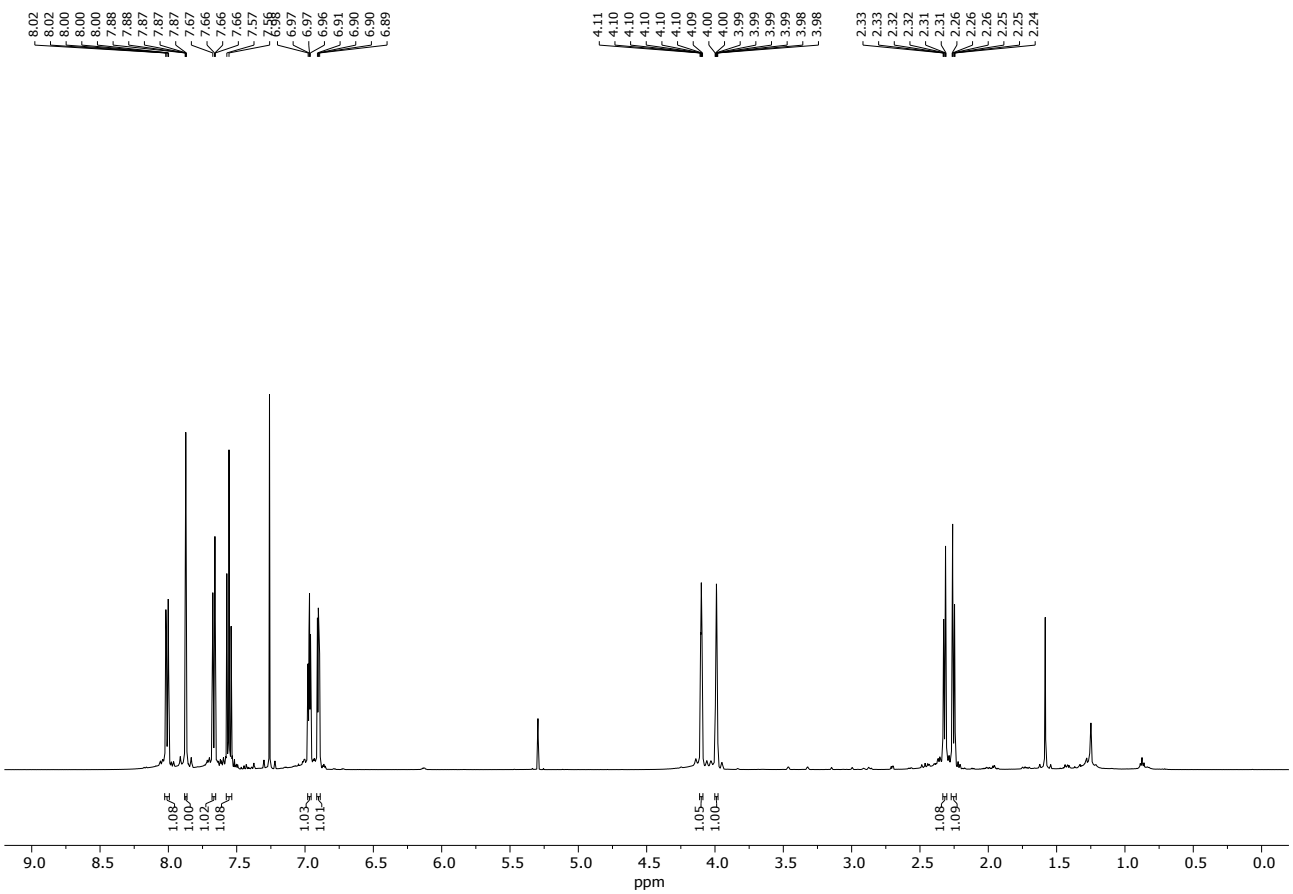

Figure S19: ^{1}H NMR (500 MHz) of **NBD18** in $CDCl_3$.

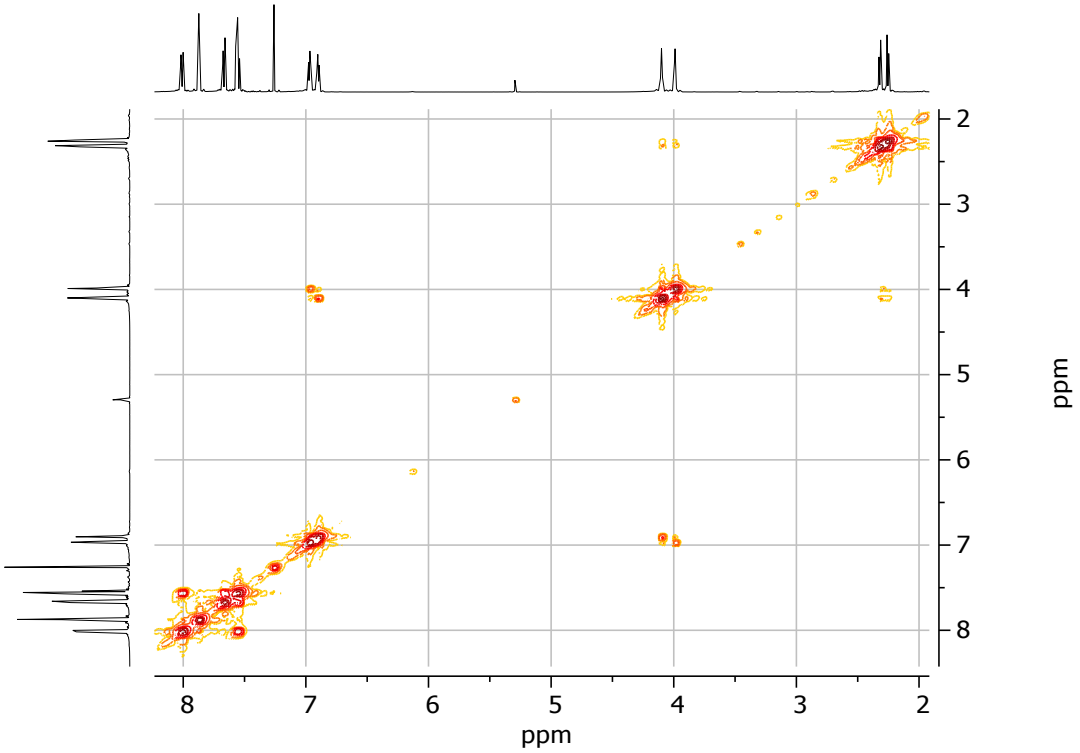

Figure S20: COSY NMR (500 MHz) of **NBD18** in $CDCl_3$.

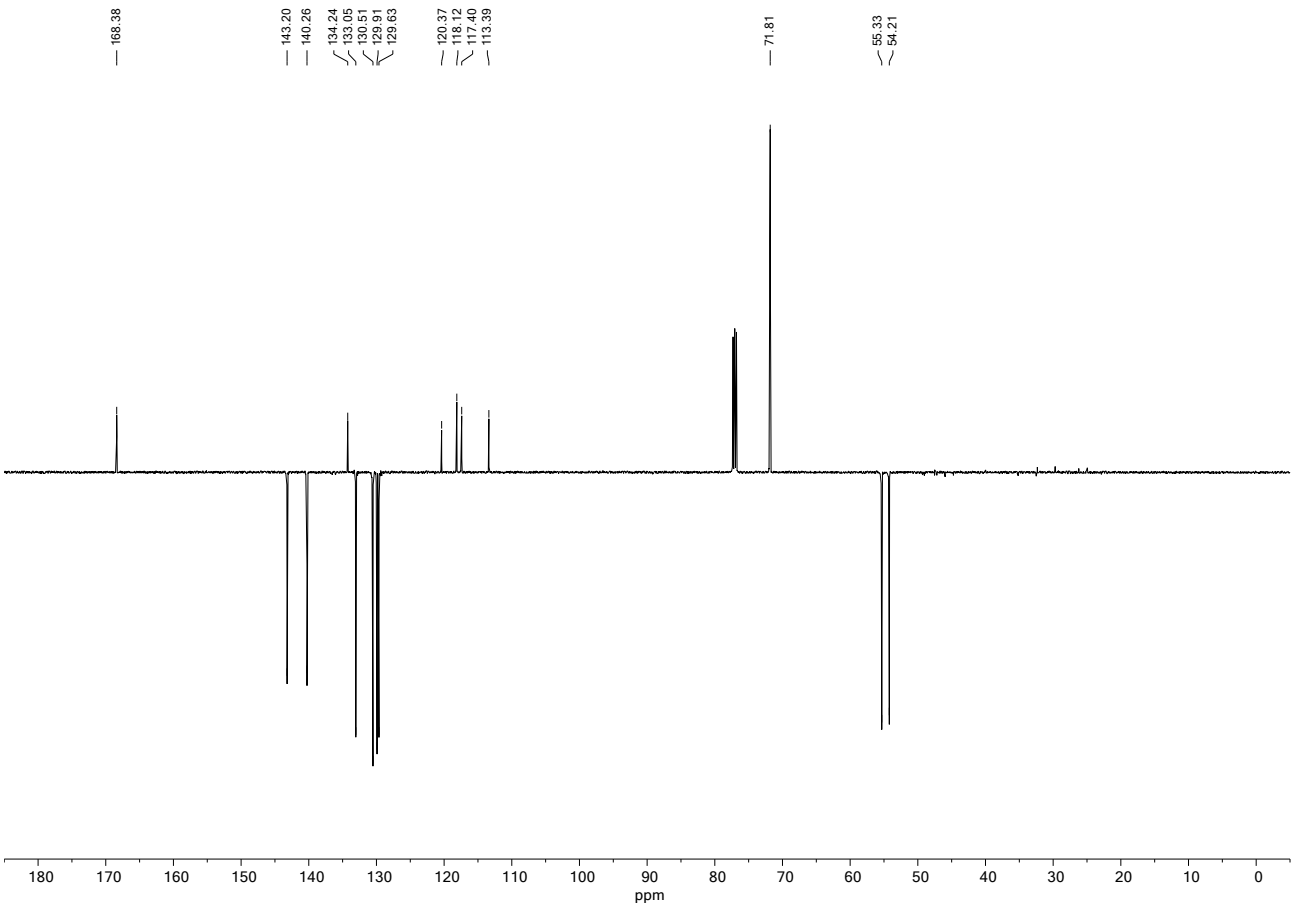

Figure S21: ^{13}C APT NMR (126 MHz) of **NBD18** in $CDCl_3$.

UV-Vis Absorption and Switching Studies (solvent: toluene)

Compound 12

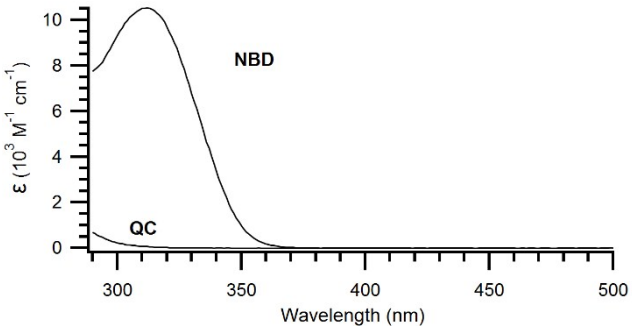

Figure S1: UV-Vis spectra of **12** and $\mathbf{12}_{QC}$.

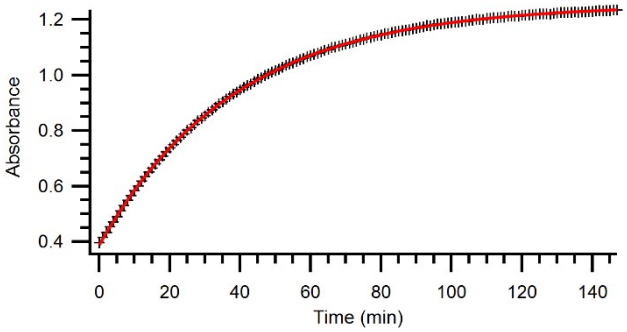

Figure S2: Increase in absorbance at 312 nm of **12** at 85 °C during the thermal backreaction.

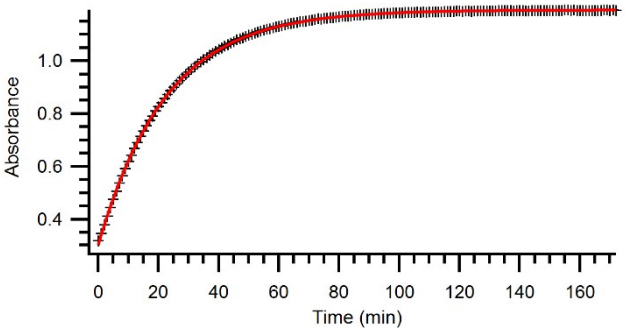

Figure S3: Increase in absorbance at 312 nm of **12** at 90 °C during the thermal backreaction.

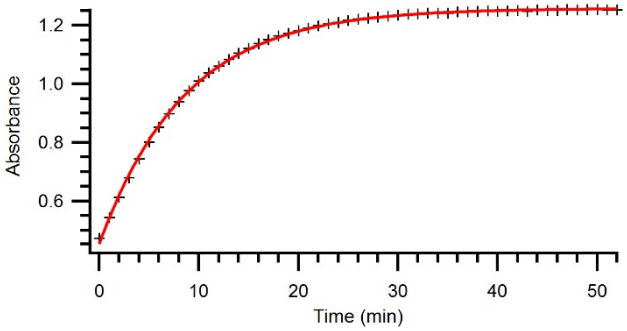

Figure S4: Increase in absorbance at 312 nm of **12** at 100 °C during the thermal backreaction.

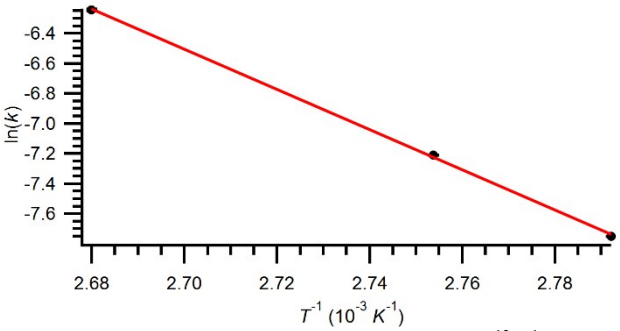

Figure S5: Arrhenius plot for **12** giving the values A = 7.00 x 10^{12} s^{-1} and E_a = 111.1 kJ/mol.

Compound 13

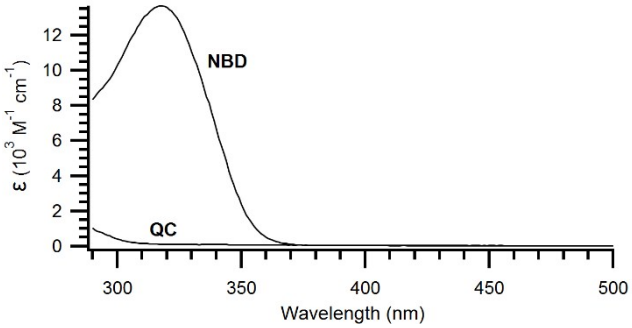

Figure S6: UV-Vis spectra of **13** and $\mathbf{13}_{QC}$.

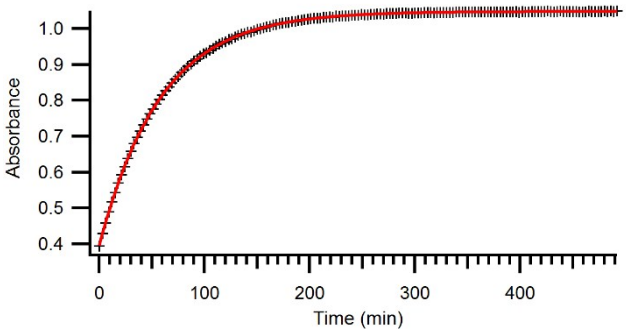

Figure S7: Increase in absorbance at 318 nm of **13** at 80 °C during the thermal backreaction.

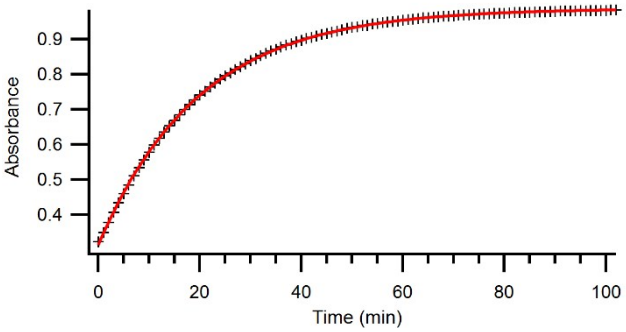

Figure S8: Increase in absorbance at 318 nm of **13** at 90 °C during the thermal backreaction.

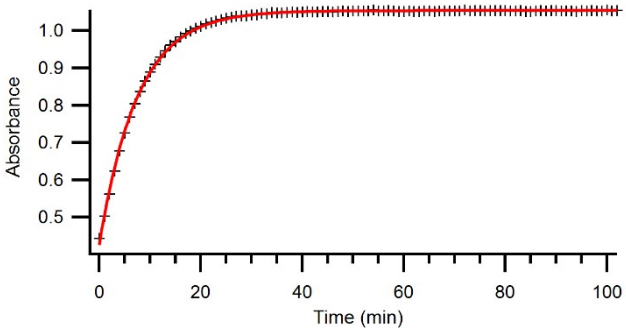

Figure S9: Increase in absorbance at 318 nm of **13** at 100 °C during the thermal backreaction.

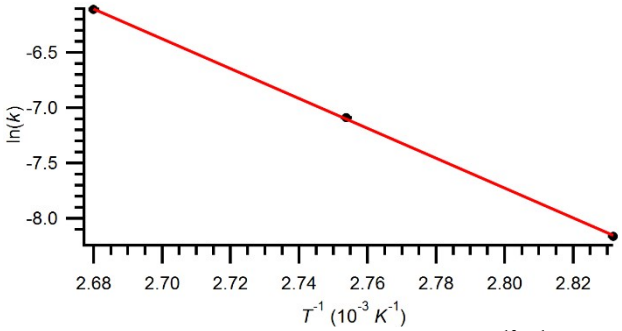

Figure S10: Arrhenius plot for **13** giving the values A = 1.13 x 10^{13} s^{-1} and E_a = 112.2 kJ/mol.

Compound 14

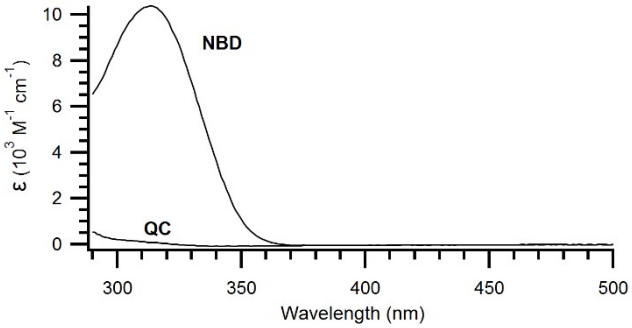

Figure S11: UV-Vis spectra of **14** and $\mathbf{14}_{QC}$.

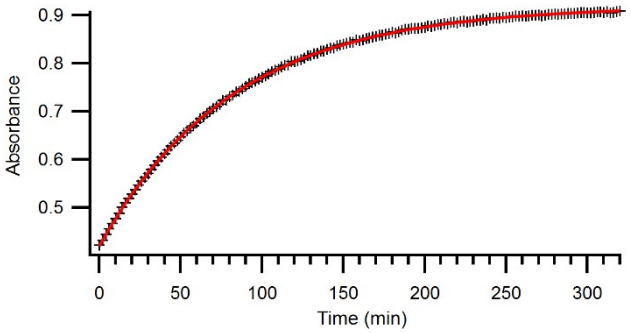

Figure S12: Increase in absorbance at 313 nm of **14** at 80 °C during the thermal backreaction.

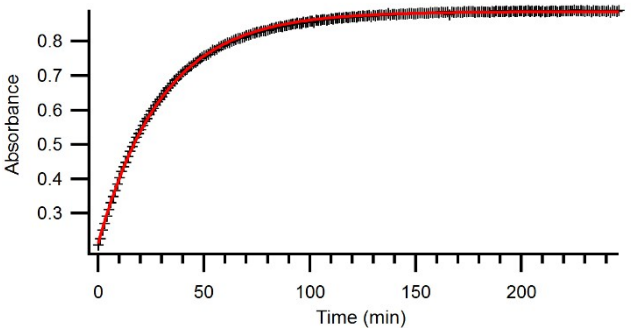

Figure S13: Increase in absorbance at 313 nm of **14** at 90 °C during the thermal backreaction.

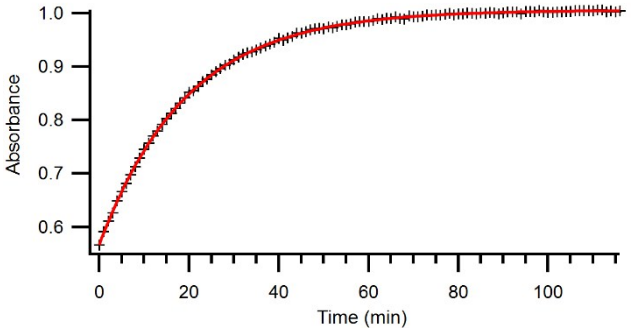

Figure S14: Increase in absorbance at 313 nm of **14** at 95 °C during the thermal backreaction.

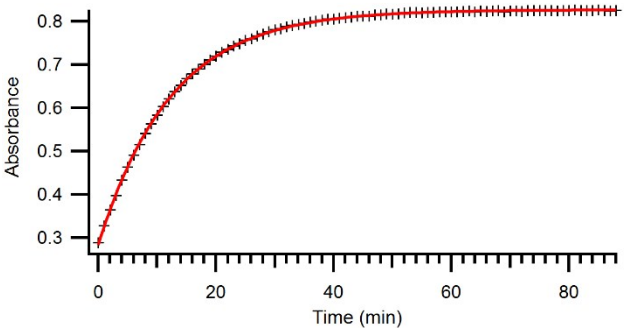

Figure S15: Increase in absorbance at 313 nm of **14** at 100 °C during the thermal backreaction.

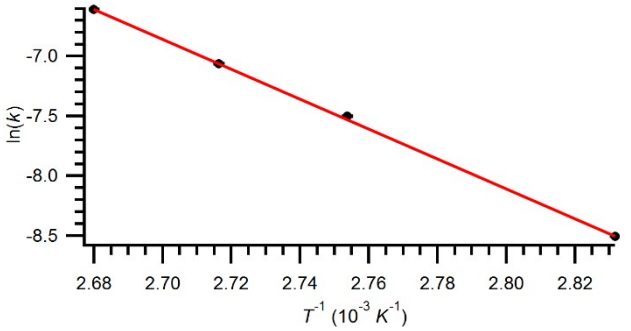

Figure S16: Arrhenius plot for **14** giving the values A = 4.62 x 10^{11} s^{-1} and E_a = 103.8 kJ/mol.

Compound 15

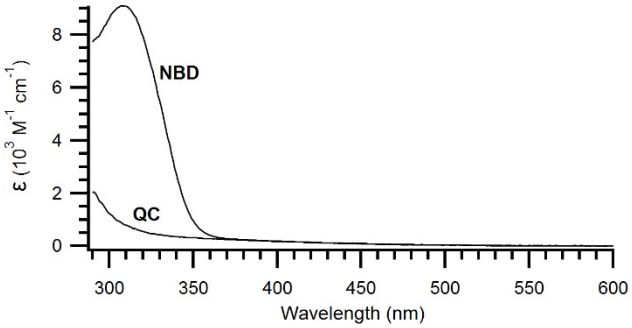

Figure S17: UV-Vis spectra of **15** and **15$_{QC}$.**

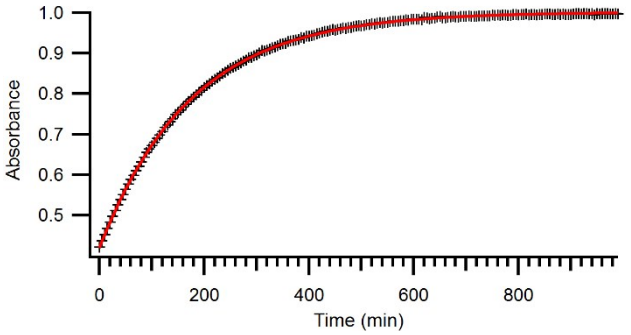

Figure S18: Increase in absorbance at 309 nm of **15** at 75 °C during the thermal backreaction-.

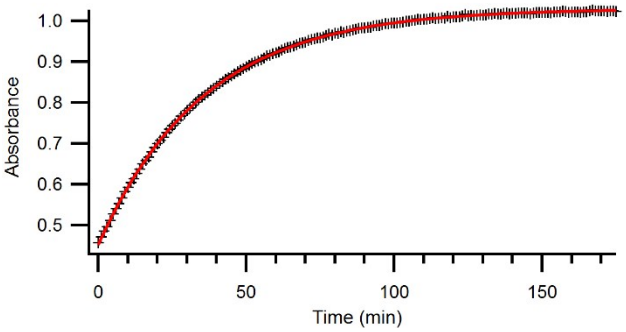

Figure S19: Increase in absorbance at 309 nm of **15** at 90 °C during the thermal backreaction-.

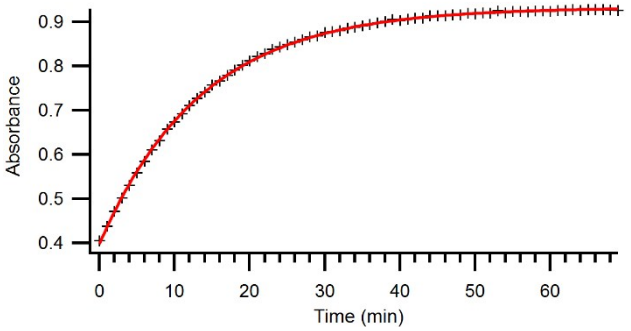

Figure S20: Increase in absorbance at 309 nm of **15** at 100 °C during the thermal backreaction-.

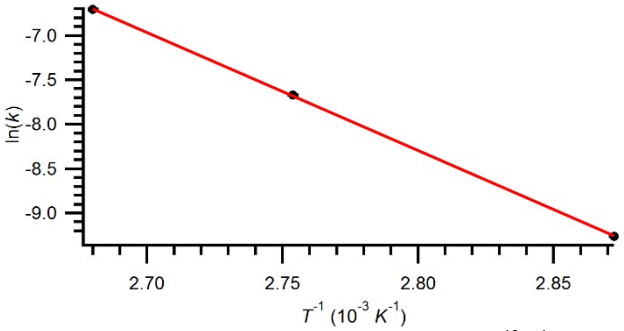

Figure S21: Arrhenius plot for **15** giving the values A = 3.55 x 10^{12} s^{-1} and E_a = 110.4 kJ/mol.

Compound 16

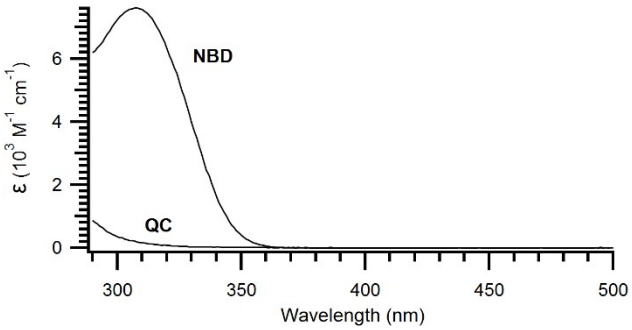

Figure S22: UV-Vis spectra of **16** and **16$_{QC}$**.

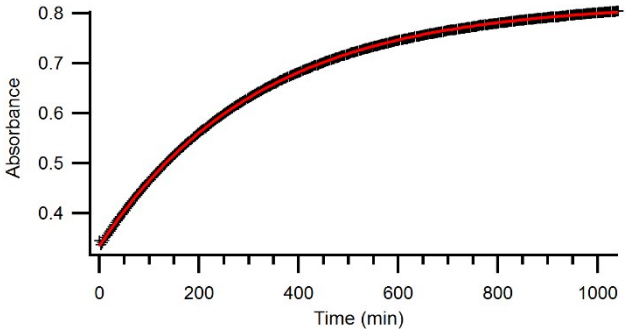

Figure S23: Increase in absorbance at 308 nm of **16** at 70 °C during the thermal backreaction.

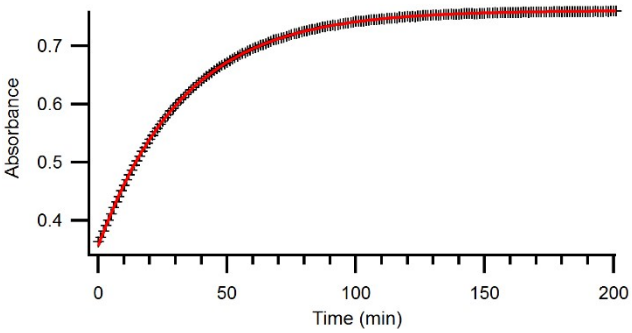

Figure S24: Increase in absorbance at 308 nm of **16** at 90 °C during the thermal backreaction.

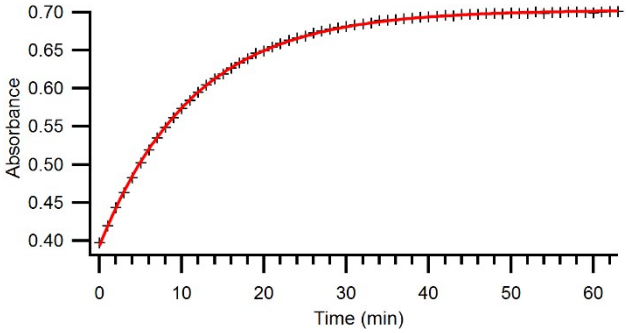

Figure S25: Increase in absorbance at 308 nm of **16** at 100 °C during the thermal backreaction.

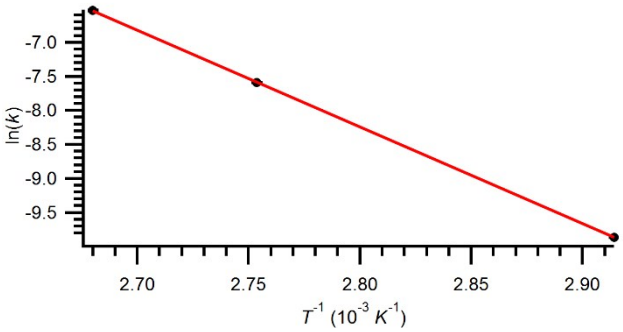

Figure S26: Arrhenius plot for **16** giving the values A =5.12 x 10^{13} s^{-1} and E_a = 118.2 kJ/mol.

Compound 17

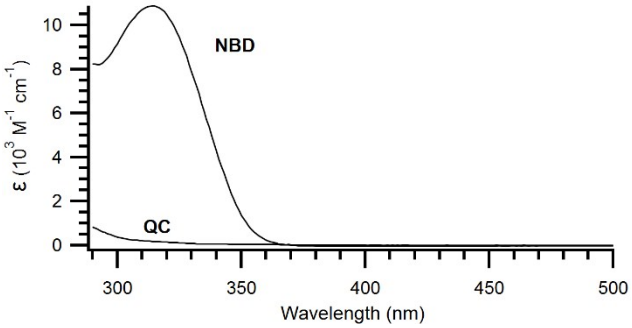

Figure S27: UV-Vis spectra of **17** and $\mathbf{17}_{QC}$.

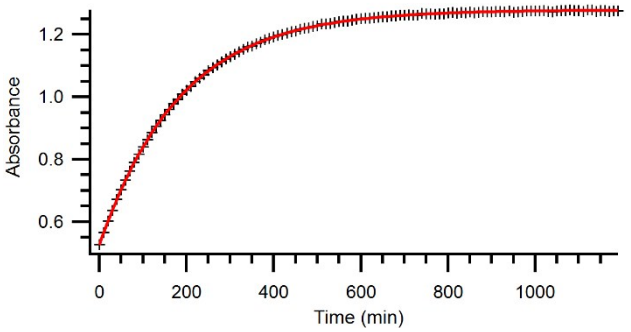

Figure S28: Increase in absorbance at 314 nm of **17** at 70 °C during the thermal backreaction.

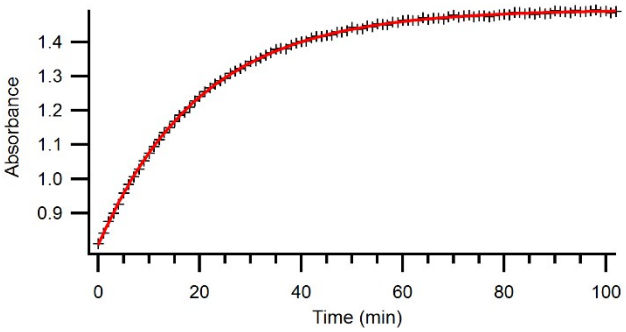

Figure S29: Increase in absorbance at 314 nm of **17** at 90 °C during the thermal backreaction.

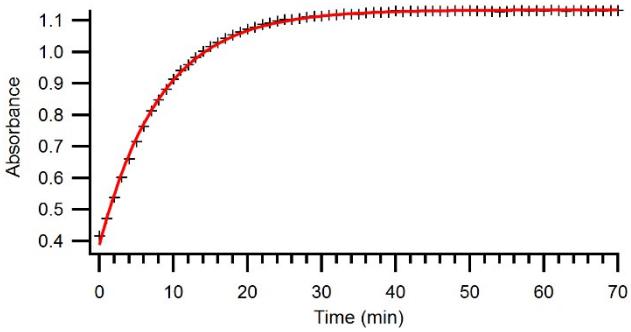

Figure S30: Increase in absorbance at 314 nm of **17** at 100 °C during the thermal backreaction.

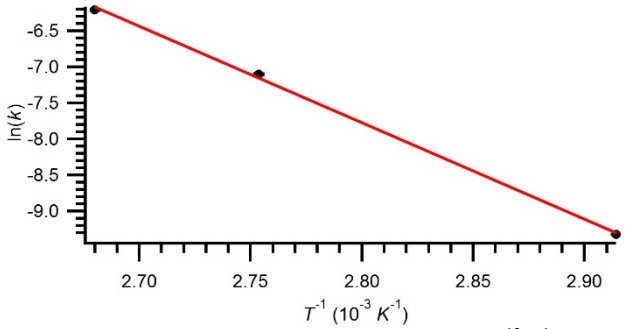

Figure S31: Arrhenius plot for **17** giving the values A = 7.58 x 10^{12} s^{-1} and E_a = 111.1 kJ/mol.

Compound 18

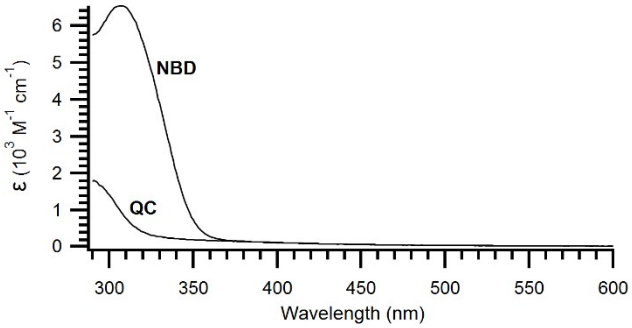

Figure S32: UV-Vis spectra of **18** and **18**$_{QC}$.

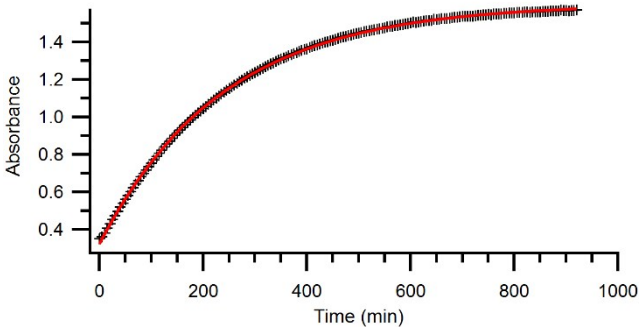

Figure S33: Increase in absorbance at 306 nm of **18** at 75 °C during the thermal backreaction.

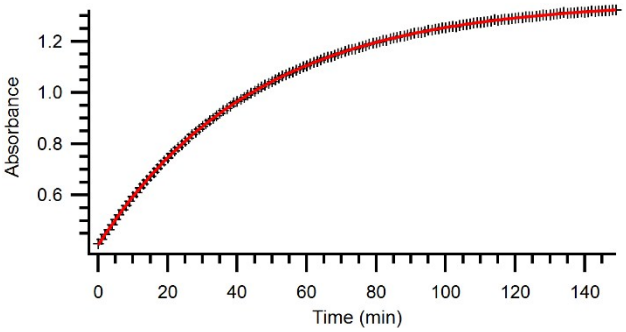

Figure S34: Increase in absorbance at 306 nm of **18** at 90 °C during the thermal backreaction.

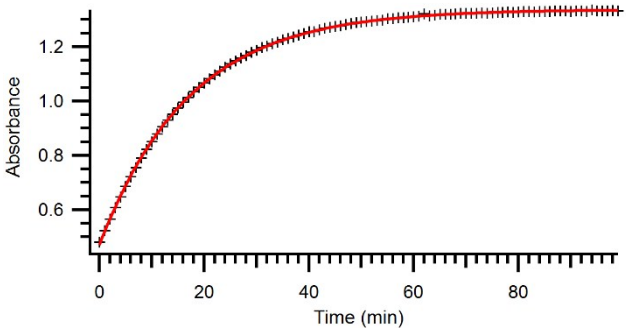

Figure S35: Increase in absorbance at 306 nm of **18** at 100 °C during the thermal backreaction.

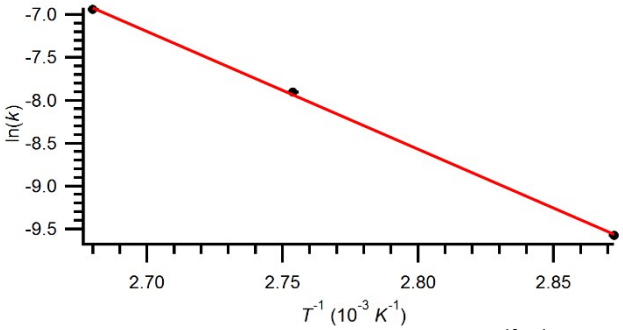

Figure S36: Arrhenius plot for **18** giving the values A = 9.41 x 10^{12} s^{-1} and E_a = 114.1 kJ/mol.

Compound 19

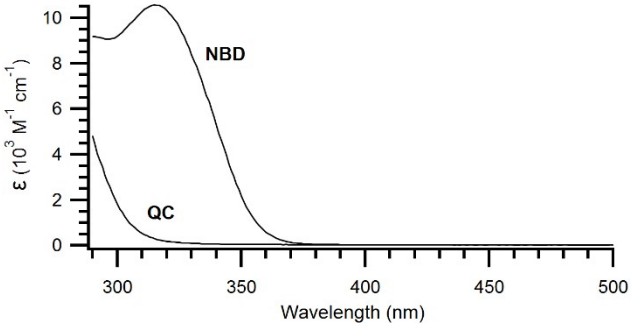

Figure S37: UV-Vis spectra of **19** and $\mathbf{19_{QC}}$.

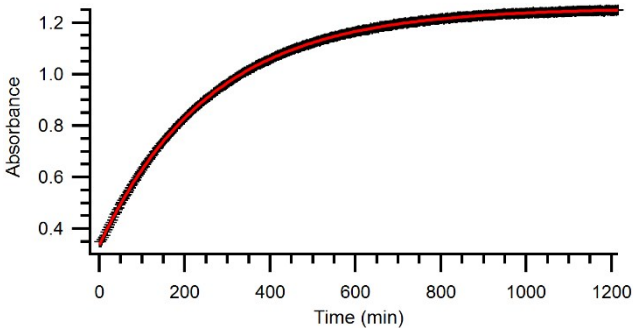

Figure S38: Increase in absorbance at 315 nm of **19** at 60 °C during the thermal backreaction.

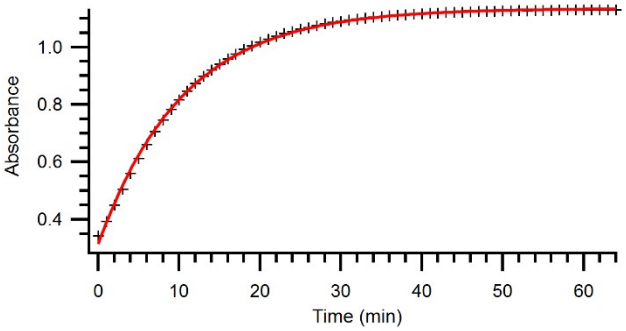

Figure S39: Increase in absorbance at 315 nm of **19** at 90 °C during the thermal backreaction.

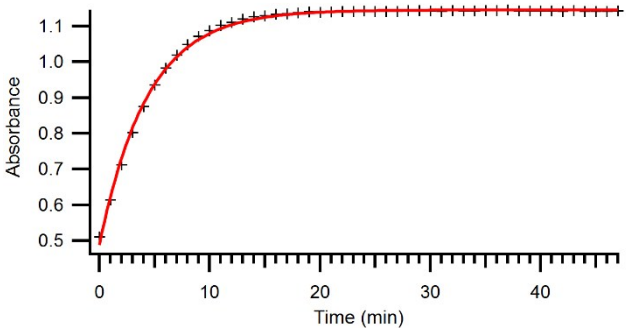

Figure S40: Increase in absorbance at 315 nm of **19** at 100 °C during the thermal backreaction.

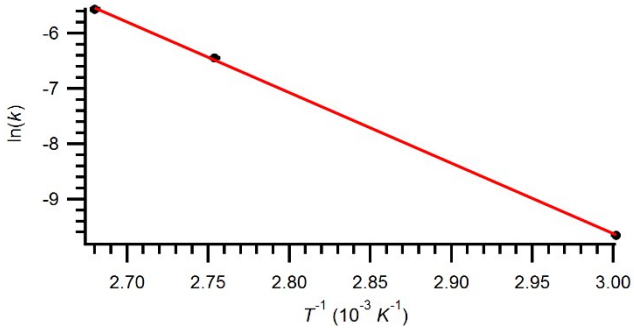

Figure S41: Arrhenius plot for **19** giving the values A = 2.90 x 10^{12} s^{-1} and E_a = 106.2 kJ/mol.

Compound 20

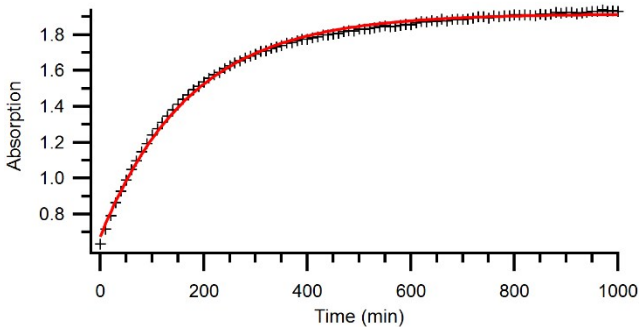

Figure S42: Increase in absorbance at 327 nm of **20** at 60 °C during the thermal backreaction.

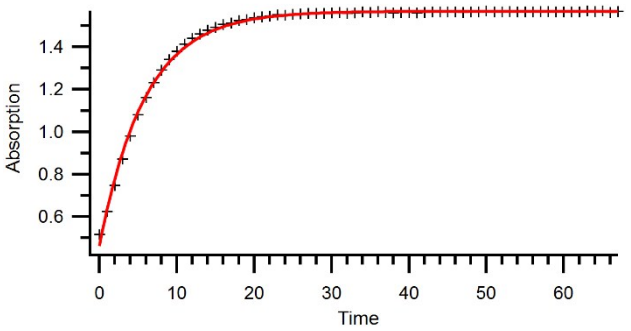

Figure S43: Increase in absorbance at 327 nm of **20** at 90 °C during the thermal backreaction.

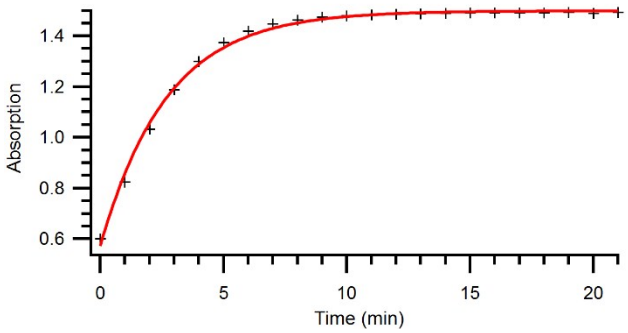

Figure S44: Increase in absorbance at 327 nm of **20** at 100 °C during the thermal backreaction.

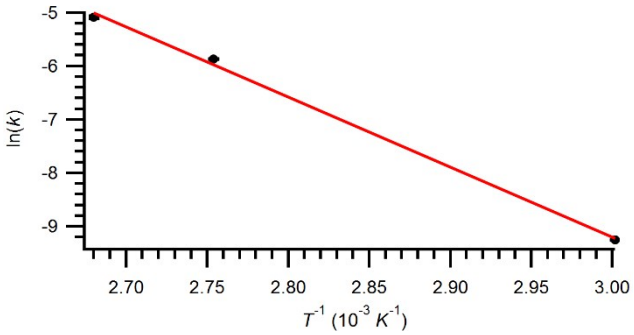

Figure S45: Arrhenius plot of **20** giving the values A = 1.21 x 10^{13} s^{-1} and E_a = 111.1 kJ/mol.

Compound 21

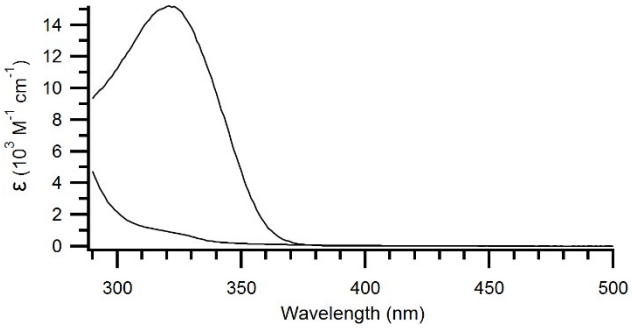

Figure S46: UV-Vis spectra of **21** and $\mathbf{21}_{QC}$.

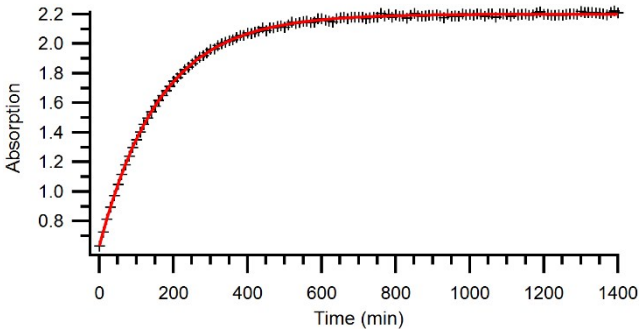

Figure S47: Increase in absorbance at 321 nm of **21** at 60 °C during the thermal backreaction.

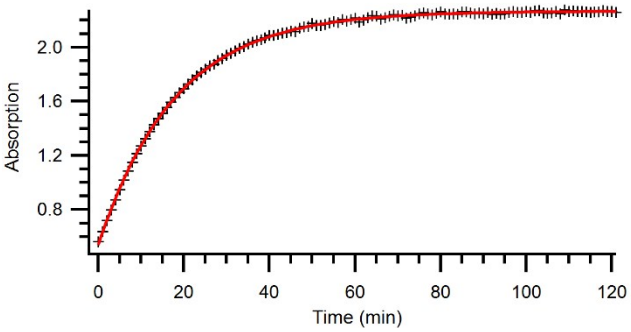

Figure S48: Increase in absorbance at 321 nm of **21** at 80 °C during the thermal backreaction.

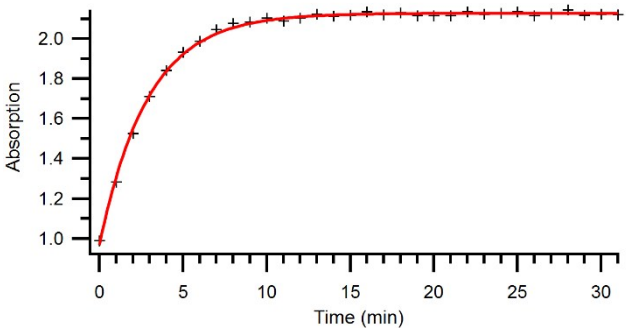

Figure S49: Increase in absorbance at 321 nm of **21** at 100 °C during the thermal backreaction.

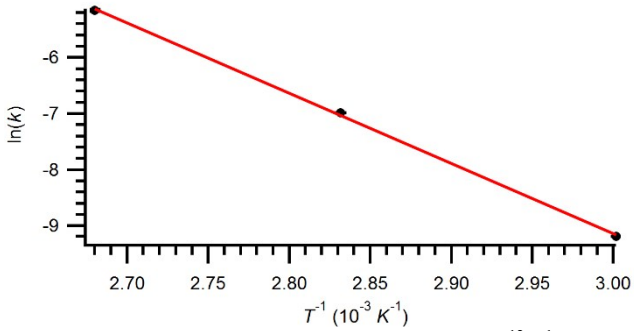

Figure S50: Arrhenius plot for **21** giving the values A = 2.23 x 10^{12} s^{-1} and E_a = 104.1 kJ/mol